

**SYSTEMS ANALYSIS OF THE GENERALIZED VERTEBRATE CONE  
RETINA, PART B. GENERATED TIME-DEPENDENT OUTPUT  
VOLTAGES FOR CONES, HORIZONTAL CELLS AND BIPOLAR CELLS**

ROBERT SIMINOFF\*

*Naval Submarine Medical Research Laboratory, Naval Submarine Base,  
New London Groton, CT 06349-0900 U.S.A.*

(Received in final form September 12, 1984)

**Abstract**

Time-dependent output voltages are generated for cones, horizontal cells and bipolar cells of the generalized vertebrate cone retina that are based on mathematical expressions derived by systems analysis using Laplace transforms. Detailed analysis of the effects of parameters such as synaptic gains, numbers of each cone-type, wave-length of light stimulus and time constants of retinal elements are made. Complex interplays of these parameters produce a diversity of response patterns for these retinal elements and bipolar cells with their antagonistic inputs of differing time courses have more complex dependencies on parameters than horizontal cells or cones. Important features in determining spatial-temporal properties of retinal elements are interplay of antagonistic inputs with differing time courses, relative dominance of cone-types, spectral distribution of stimuli, and negative feedback from horizontal cells to cones. Results of the model are compared with physiological data.

**1. Introduction**

In the preceding paper, systems analysis in conjunction with Laplace transforms ( $L\{s\}$ ) were applied to a model of the generalized vertebrate cone retina and expressions for time-dependent output voltages  $[F(t)]$  were derived for cones (PC), horizontal cells (HC), and bipolar cells (BC) (Siminoff, 1984*d*); this paper will be referred to as Part A. This model contains such features as color-coding or chromaticity (C-), non-color-coding or luminosity (L-), and also negative feedback from L-type HC's to PC's. Dynamic characteristics of the retina are determined mainly by negative feedback loops, which have 4 elements with differing time courses (i.e. the 3 cone-types and L-HC). Depending on the gains of negative feedback ( $K_2$ ) and PC/HC synapse ( $K_3$ ),  $F(t)$ 's varied from linear cascading of 4 exponential curves to linear cascading of 2 damped sine waves.

The present paper is Part B of this series and deals with  $F(t)$ 's generated by the mathematical expressions (see Tables 4, 8 and 9 of Part A). Parameters such as synaptic gains ( $K_i$ ), intensity factors for the stimuli ( $W_x$ ) and time-constants ( $T_x$ ) are varied and results are discussed in relationship to the generalized model.

\*Present address: 705 Sycamore Terrace, DeWitt, NY 13214, U.S.A.

## 2. Parameters

A number of parameters are involved with determining  $F(t)$ 's for retinal elements and each can be varied. These parameters are divided into 3 categories (Table 1), gain factors, intensity factors and time constants. Synaptic gains are simple linear transfer functions and the same values are used as in an electronic simulation (Siminoff, 1983a). Intensity factors ( $Y_x$ ) determine input voltages from simulated cones to cone pedicles. The output voltages from the simulated cones of the electronic model were measured in response to various intensities of light stimuli and are used as the intensity factors  $Y_x$ ;  $Y_x$  therefore, represents the output voltage of a given cone-type to a given light intensity taking into account Invariance and stray light. The numbers of cones ( $N_x$ ) in the unit hexagon are those from the "trichromatic" retina (Siminoff, 1980a).

Table 1. Definition of parameters.

Parameter	Definition	Values used in text					
<b>A. Gain factors</b>							
$K_1$	Cone/PC interface	0.24					
$K_2$	L-HC/PC synapse	0 to 1.0					
$K_3$	PC/HC synapse	0 to 1.0					
$K_4$	L-HC/C-HC synapse	0 to 1.0					
$K_5$	PC/BC synapse	0 to 1.0					
$K_6$	C-HC/C-BC synapse	0 to 1.0					
$K_8$	L-HC/L-BC synapse	0 to 1.0					
<b>B. Intensity factors</b>							
$N_R$	# red cones to PR	9					
$N_G$	# green cones to PG	6					
$N_B$	# blue cones to PB	4					
		WL	RL	YL	GL	BL	
$Y_R$	input voltage to PR	88.50	9.04	8.71	2.90	3.24	
$Y_G$	input voltage to PG	88.10	10.21	11.22	5.51	5.46	
$Y_B$	input voltage to PB	77.27	9.27	9.82	4.98	5.28	
$W_R$	$N_R Y_R$						
$W_G$	$N_G Y_G$						
$W_B$	$N_B Y_B$						
<b>C. Time constants</b>							
$T_R$	for PR	0.09 sec					
$T_G$	for PG	0.10 sec					
$T_B$	for PB	0.14 sec					
$T_C$	for other elements	0.047 sec					
$J$	$1/T_R$	11.111 sec <sup>-1</sup>					
$K$	$1/T_G$	10.000 sec <sup>-1</sup>					
$L$	$1/T_B$	7.1426 sec <sup>-1</sup>					
$G$	$1/T_C$	21.2766 sec <sup>-1</sup>					

Table 1A. Coding of parameter values used for labelling curves of Figures.

Label	$K_2$	$K_3$	$K_4$	$K_5$	$K_6$ or $K_8$	$W_r$	$W_g$	$W_b$	
1	—	1	0	—	—	796.59	528.6	309.08	
2	—	1	0.25	—	—	796.59	528.6	309.08	
3	—	1	0.50	—	—	796.59	528.6	309.08	
4	—	1	0.75	—	—	796.59	528.6	309.08	
5	—	1	1	—	—	796.59	528.6	309.08	
6	—	0.75	1	—	—	796.59	528.6	309.08	
7	—	0.50	1	—	—	796.59	528.6	309.08	
8	—	0.25	1	—	—	796.59	528.6	309.08	
13	—	1	0.25	1	0.1	81.32	61.26	29.07	(RL)
14	—	1	0.25	1	0.1	26.14	33.04	19.08	(GL)
15	—	1	0.25	1	0.1	28.99	32.74	20.82	(BL)
16	—	1	0.25	1	0.1	78.39	25.32	39.27	(YL)
17	—	1	0	—	—	796.59	528.6	0	
18	—	1	0	—	—	796.59	0	309.08	
19	—	1	0	—	—	0	528.6	309.08	
20	—	1	0	—	—	796.59	0	0	
21	—	1	0	—	—	0	528.6	0	
22	—	1	0	—	—	0	0	309.08	
23	—	1	0.25	1	0.1	796.59	528.6	0	
24	—	1	0.25	1	0.1	796.59	0	309.08	
25	—	1	0.25	1	0.1	0	528.6	309.08	
26	—	1	0.25	1	0.1	796.59	0	0	
27	—	1	0.25	1	0.1	0	528.6	0	
28	—	1	0.25	1	0.1	0	0	309.08	
29	—	1	0.25	1	0.1	796.59	528.6	309.08	
30	0	variable	1	—	—	796.59	528.6	309.08	
31	0.05	variable	1	—	—	796.59	528.6	309.08	
32	0.25	variable	1	—	—	796.59	528.6	309.08	
33	100	variable	1	—	—	796.59	528.6	309.08	
34	0	1	variable	—	—	796.59	528.6	309.08	

### 3.1 Cone Pedicles

#### Introduction

Three cone-types are used, red (PR), green (PG) and blue (PB) with time constants  $T_r$ ,  $T_g$  and  $T_b$ , respectively (Table 1). The unit hexagon (UH) defines the cone input to the center field of a BC or to a HC and each UH has associated with it a PR, a PG and a PB. The PC acts as a summing point for cone inputs to the BC or HC, and the specific numbers of each cone-type as listed in Table 1 result from the "trichromatic" mosaic (Siminoff, 1980a). Time constants listed in Table 1 are those used in the electronic model and are somewhat arbitrary, although approximating those of lower vertebrates, but differences are exaggerated to show the effects of differing time constants. Mammalian retinas probably have lower values of  $T_x$  for cones.

### Effects of varying negative feedback ( $K_2$ ) with $K_3=1$

With  $K_2=0$ ,  $PX(t)$ 's have typical exponential waveforms with  $PR(t)$  having the fastest (Fig. 1A),  $PG(t)$  an intermediate (Fig. 1B), and  $PB(t)$  the slowest (Fig. 1C) time

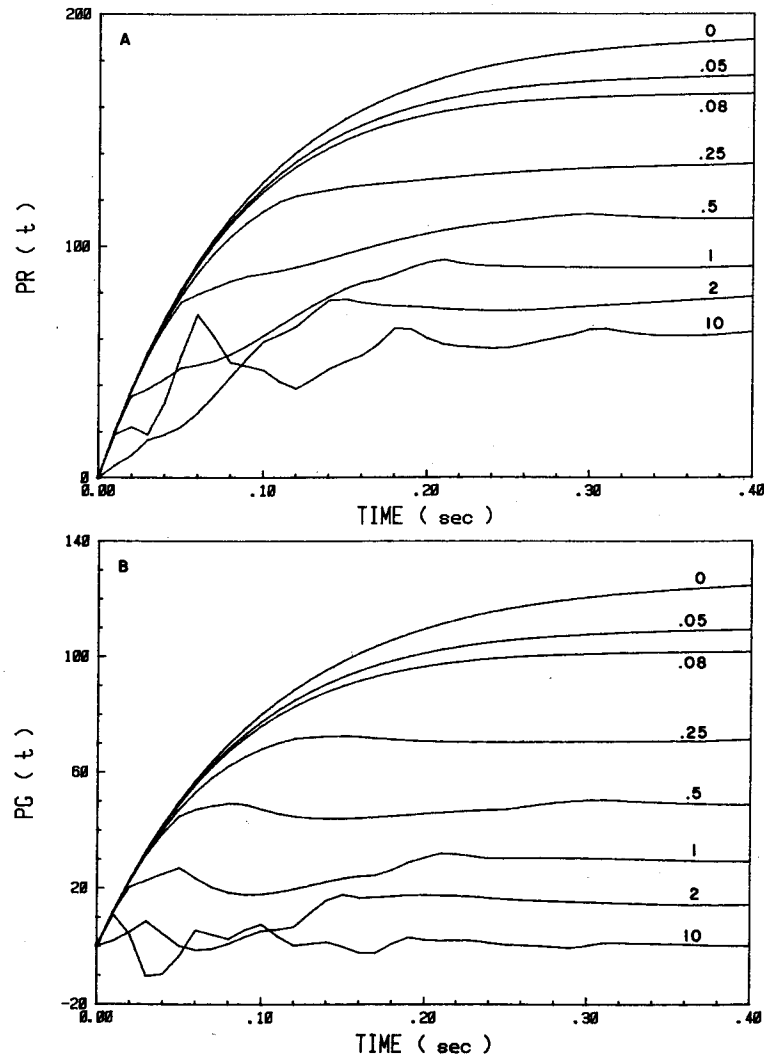


**Fig. 1.** Generated output voltages for PC's evoked by white light. Numbers used to designate curves for A, B and C are values of  $K_2$  with  $K_3=1$ . A, B and C display  $F(t)$ 's for red (PR), green (PG) and blue (PB) PC's, respectively. D displays  $PC(t)$ 's with  $K_2=0.25$ . Refer to Table 1A for this and for subsequent figures for values of parameters designated by numbers used to label curves. The x-axis is time after start of a step input voltage. These and all subsequent curves are constructed by a computer, programmed to connect Y-values that are 0.01 sec apart.

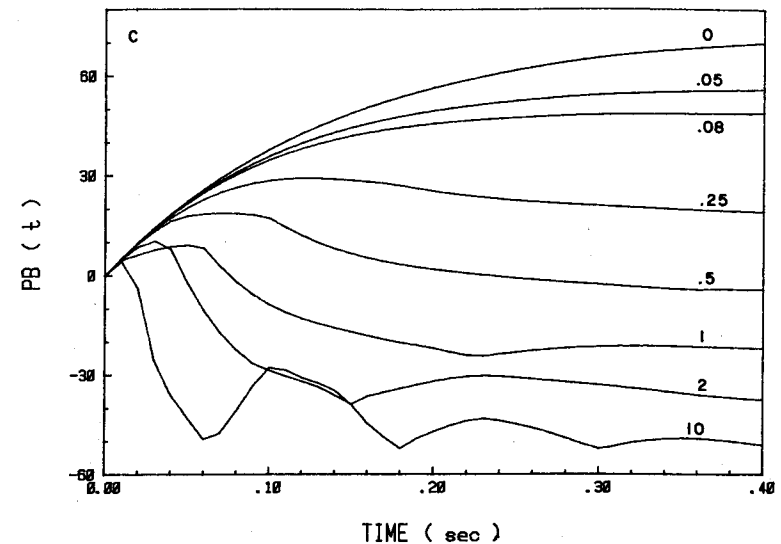


Fig. 1 continued

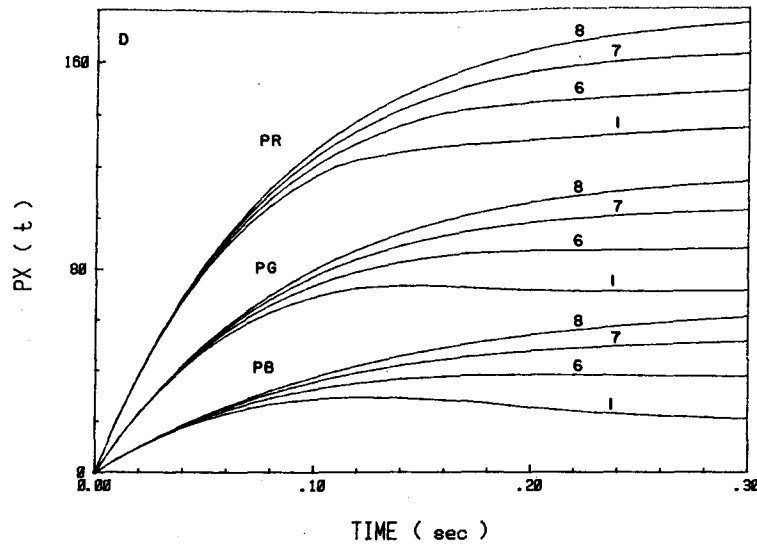
course. Since  $F(t)$ 's reflect the numbers of cones ( $N_c$ ) acting as input and intensities ( $Y_c$ ),  $PR$  has the largest, while  $PB$  has the smallest response to white light. Below the 1st critical value of  $K_2K_3$ , which is about 0.0520,  $PX(t)$ 's are typically exponential, while above the 2nd critical value of 0.0775,  $PX(t)$ 's are damped sine waves, although this is not readily apparent until  $K_2=10$ . With  $K_2=0.25$ ,  $PR(t)$  displays a flattening which starts at about 0.1 sec and lengthens as  $K_2$  is increased: with  $K_2$  equal to or greater than 0.5 a damped sine wave appears on the flat portion of the curve (Fig. 1A). With  $PG(t)$  and  $PB(t)$  and with  $K_2=0.25$ , slight overshoots appear at about 0.12 (Fig. 1B, C) instead of the flattening seen with  $PR(t)$ , and with  $K_2=0.5$  for  $PG(t)$  and one for  $PB(t)$  the damped sine waves are readily discernible.  $PG(t)$ 's and  $PB(t)$ 's become greatly decreased with increasing values of  $K_2$ , such that after the initial positive overshoots, the curves swing negative with  $K_2=10$  for  $PG(t)$  and  $K_2$  greater than 0.5 for  $PB(t)$ .

### Effects of varying PC/HC synaptic gain ( $K_3$ ) with $K_2=0.25$

The waveforms of  $PX(t)$  approach those of pure exponential curves as  $K_3$  decreases (Fig. 1D) which is consistent with the effects of decreasing  $K_2$  (Fig. 1A-C), since the amount of negative feedback depends on  $K_2K_3$  as shown in part A.

### Effects of different colored lights on $PX(t)$ 's

Red and yellow colored lights evoked responses for  $PR$  (Fig. 2A) that are similar to those evoked by white light (Fig. 1A), although the initial phases are flatter. Green and



blue colored lights evoked responses in PR that are more like those evoked by white light for PG (Fig. 1B) and PB (Fig. 1C). With green and blue colored lights,  $PG(t)$ 's show some flattening (Fig. 2B), while responses to red and yellow colored lights are more like the responses of PG and PB to white light. All  $PB(t)$ 's evoked by colored light stimuli (Fig. 2C) are like the responses of PG evoked by green or blue colored lights except that the initial phases at about 0.15 sec are exaggerated, particularly those evoked by red and yellow colored lights.

*Effects of varying the number of cones ( $N_x$ )*

When direct cone input voltages are present,  $F(t)$ 's are positive, but when direct cone input voltages are absent (i.e. the respective  $N_x$  is zero),  $F(t)$ 's are negative and have slower time courses (Fig. 2D-F).  $PR(t)$ 's increase (i.e. become more positive) when green or blue cone input voltages are eliminated (Fig. 2D).  $PR(t)$  is maximal (Fig. 2D) when only the direct red cone input voltages are present, but is somewhat flattened indicating the presence of feedback loops (see Fig. 2A of Part A). With no direct red cone input voltages,  $PR(t)$ 's are negative and green cone activation is more effective than blue cone activation, while blue+green cones activation gives the maximum negative response. The effects of elimination of cone inputs to PG (Fig. 2E) are similar to the effects on PR except that the direct cone input is now green. A major difference between the effects of cone elimination on PR and PG is the presence of an initial overshoot seen with  $PG(t)$  when red and green cones are activated (Fig. 2E), but with the absence of red cone activation flattening occurs with green or green + blue cones activation.  $PB(t)$  does not show any discernible flattening when only blue cones are activated (Fig. 2F) and responses are larger with green than red cone activations.

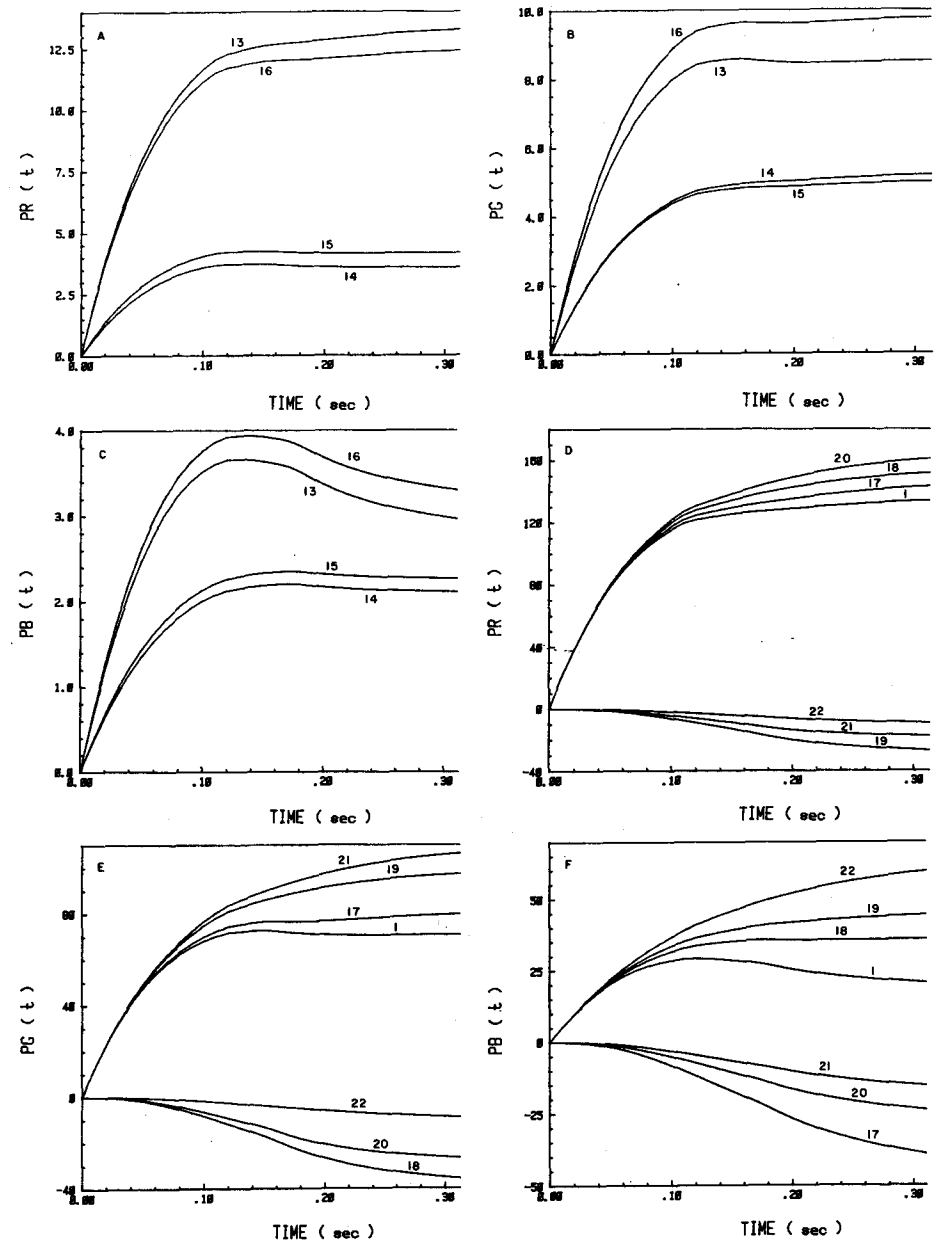


Fig. 2. Generated output voltages for PC's evoked by colored lights or with altered numbers of cones with  $K_2=0.25$ . A, B and C portray  $PC(t)$ 's evoked by different colored lights. D, E and F display  $PC(t)$ 's evoked by white light, but with indicated cone-types having  $N_x=0$ .

### 3.2 Horizontal Cells (HC)

There are 2 types of HC's: C-HC, which is color-coded, and L-HC, which is non-color-coded. L-HC is formed by direct input voltages from all 3 cone-types. C-HC has only one (or 2 for yellow) direct cone input voltages with gains of  $K_3$ , and an antagonistic input voltage from L-HC with a gain of  $K_4$ .

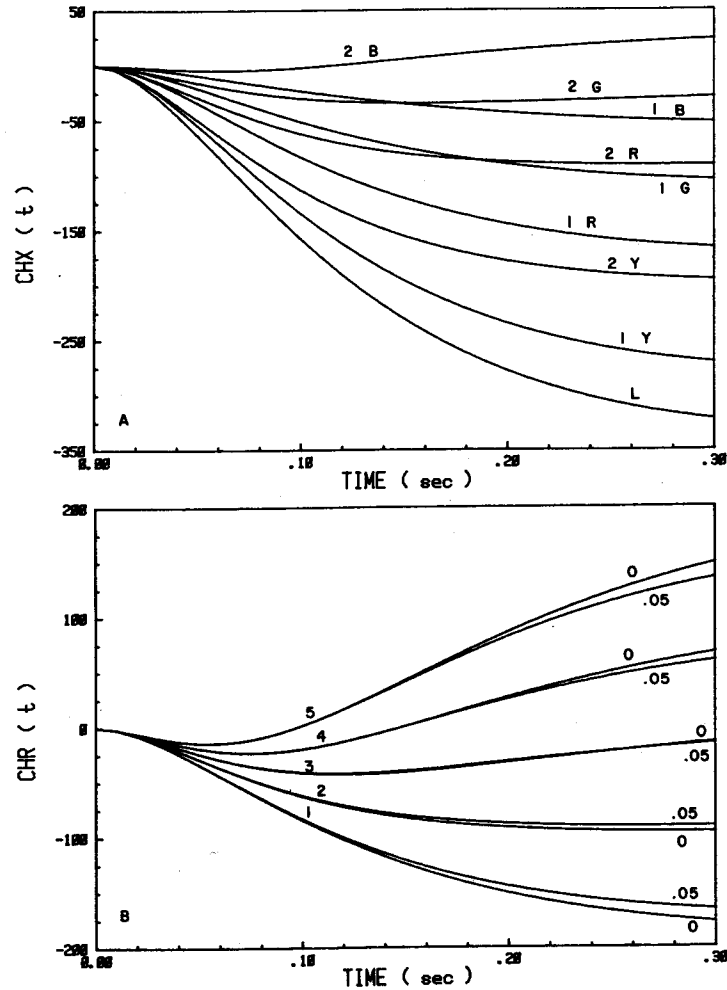


Fig. 3. Generated outputs voltages for HC's evoked by white light. A displays  $CHX(t)$ 's with varied amounts of input voltage from L-HC ( $K_4$ ) at  $K_2=0.25$ . Letters used to designate curves along with numbers indicate type of HC, i.e. L=L-HC, R=C-HR, G=C-HG, B=C-HB and Y=C-HY.  $K_2=0.05$ . B and C display  $CHR(t)$ 's with varied amounts of  $K_4$  keeping  $K_3$  constant. For each value of  $K_4$ , there are 2 curves, i.e.  $K_2=0$  and  $K_2=0.05$ . D displays  $CHR(t)$ 's of B and C with time scale expanded to give details of transient phases.

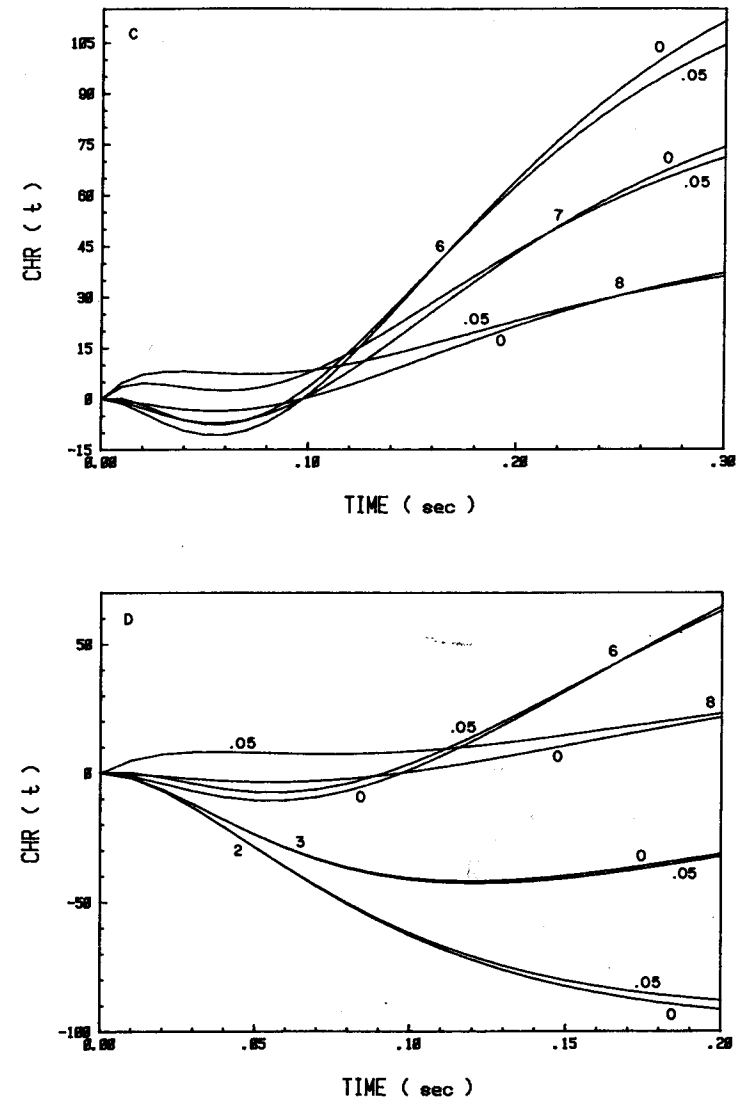


Fig. 3 continued

#### Effects of L-HC input voltage with gain $K_4$ on $CHX(t)$ 's

With negative feedback below the critical value of  $K_2K_3=0.050$  and with  $K_4=0$ , the waveform of all  $HC(t)$ 's are typical exponential curves (Fig. 3A) with time courses dictated by the time constants ( $T_c$ ) of the direct cone input voltages: therefore,  $CHR(t)$

has the fastest and CHB( $t$ ) has the slowest time courses. CHY( $t$ ) and LH( $t$ ), which have predominately red cone input voltages, have similar time courses as that of CHR( $t$ ). Adding input voltages from L-HC to C-HC's (i.e.  $K_4$ ) introduces antagonistic input voltages with slower time courses than those of the direct input voltages. Thus, the effects of L-HC input voltages to C-HC's (as typified by C-HR) are not apparent until a short delay (Fig. 3A, B). Increasing L-HC input voltages to C-HC's causes a shift in steady state levels ( $F_{ss}$ ) from negative to positive values after a brief delay of about 0.04–0.05 sec. Decreasing the direct cone input voltages (i.e. by decreasing  $K_3$ ) to the HC's has the opposite effect, i.e. causing a shift of  $F_{ss}$  back towards the negative level after a short delay of 0.05 to 0.06 sec (Fig. 3C, D). When one of the direct cone input voltages dominates, increasing  $K_2$  from 0 to 0.05 has no effect on the initial slope (Fig. 3B), but causes  $F_{ss}$ 's to shift towards the positive level if  $K_4$  is low, and towards the negative level if  $K_4$  is greater than 0.5. At  $K_4=0.5$ , the curves for  $K_2=0$  and for  $K_2=0.05$  are nearly identical. When the L-HC input voltage to C-HC dominates (Fig. 3C, D), increasing  $K_2$  from 0 to 0.05 produced marked effects on the initial slope as well as on  $F_{ss}$  (Fig. 3C, D), thereby, causing the curves to shift initially towards the positive level and then towards the negative level after variable delays of about 0.17 sec for  $K_3=0.75$  and 0.24 sec for  $K_3=0.25$  (Fig. 3D). Increasing negative feedback produces an initial positive notch on CBX( $t$ ) that arises as a result of the action of the slower antagonistic L-HC input voltage.

#### Effects of L-HC input voltage on CHX( $t$ ) with $K_2K_3$ above the critical level

The 2nd critical level is exceeded when  $K_2K_3=0.25$ , so that  $F(t)$ 's are described by damped sine waves. For LH( $t$ )'s the initial negative slopes, which reflect exponential curves, are broken at about 0.19 sec by positive waves that peak at about 0.34 sec and then asymptote to negative values of  $F_{ss}$ 's (Fig. 4A). Changing  $K_4$  has no effect on LH( $t$ ) since  $K_4$  is not one of the parameters determining LH( $t$ ) (see Part A). However, when  $K_3$  is decreased, there is a two-fold effect, (a) the produce  $K_2K_3$  is decreased, and (b) the overall values of LH( $t$ )'s are decreased. Decreasing  $K_3$  leads to a decrease in the amplitude of LH( $t$ ) as well as decreasing the late positive wave (Fig. 4A) that arises due to oscillations in the delayed sine wave. Since C-HC's responses differ only as to relative time courses and intensity factors, only CHG( $t$ )'s are shown (Fig. 4B), but these curves are representative of the others. With no L-HC input voltage (i.e.  $K_4=0$ ), CHX( $t$ )'s are quite similar to the curves for L-HC. Adding a L-HC input voltage (i.e. increasing  $K_4$ ) introduces an initial large positive overshoot which peaks at 0.06–0.07 sec (Fig. 4B). Decreasing  $K_3$ , and thereby, negative feedback, decreases both the initial positive overshoot as well as the positive shift in  $F_{ss}$ . Thus, the positive overshoots originate from the slower antagonistic input voltages.

#### Effects of colored lights on evoking HC( $t$ )'s

The basic wave shapes of LH( $t$ ) and CHX( $t$ )'s evoked by colored lights are unaltered and only overall levels, which are dependent on relative intensity factors ( $W_c$ ), are affected (Table 2). With  $K_2K_3=0.25$ , the positive peaks of all 4 C-HC's are evoked most effectively by yellow light and least effectively by green light. The

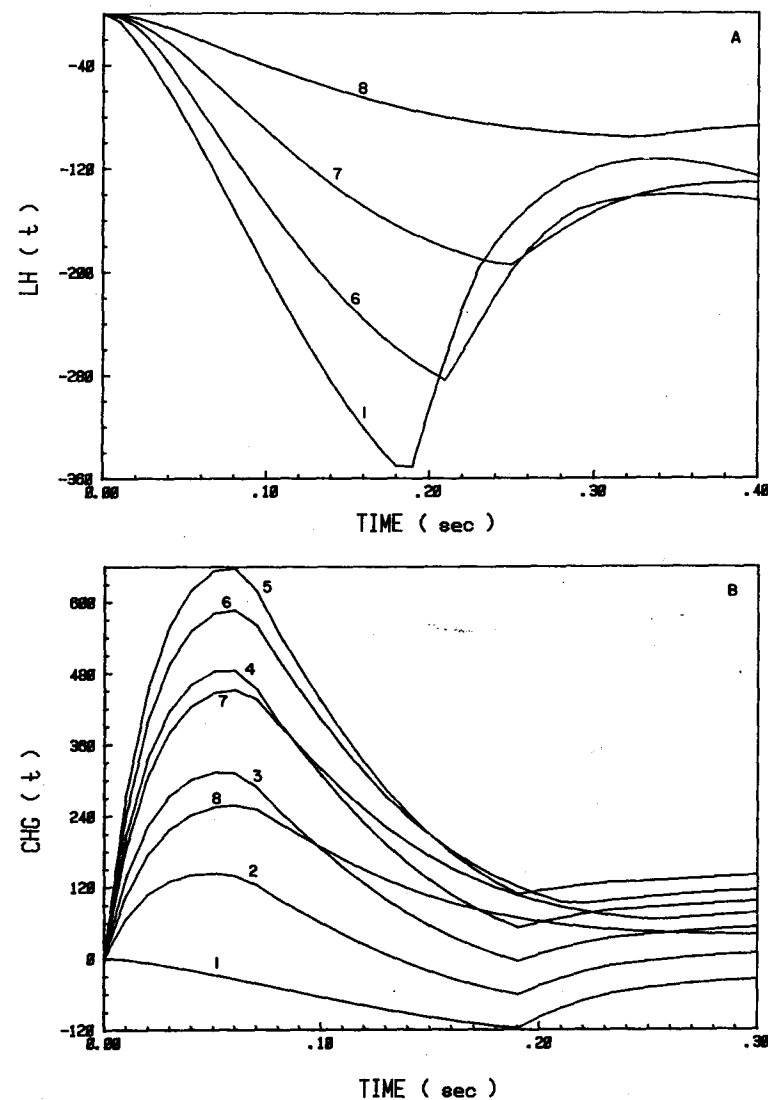


Fig. 4. Generated output voltages for HC's with  $K_2=0.25$ . A and B display LH( $t$ )'s and CHG( $t$ )'s, respectively. Note that only initial portions of  $F(t)$ 's are shown in order to see details of transient phases. Curves here as in all figures approach smoothly their steady state values once past last indicated time (i.e. 0.2–0.4 sec).

negative peaks of LH( $t$ )'s evoked by colored lights have the same order of effectiveness as does the early positive peaks of CHX( $t$ )'s. For HC's, those colored lights that are most effective in evoking the direct cone input voltages give the largest

Table 2. Relative effectiveness of colored lights to evoke HC(t)'s.

CHX(t)	Peak				$F_{ss}$			
	YL	RL	GL	BL	YL	RL	GL	BL
LH	-39.68 (0.19)	-38.53 (0.19)	-16.94 (0.19)	-17.76 (0.19)	-18.68	-18.12	-8.03	-8.43
CHR	+15.65 (0.05)	+15.05 (0.04)	+6.97 (0.05)	+7.24 (0.05)	-3.38	-4.31	+0.01	-0.33
CHG	+15.68 (0.05)	+15.45 (0.05)	+6.41 (0.05)	+6.82 (0.05)	-1.34	-0.48	-1.42	-1.10
CHB	+16.74 (0.05)	+16.39 (0.05)	+6.92 (0.05)	+7.30 (0.05)	+3.78	+3.89	+0.97	+0.97
CHY	+13.08 (0.04)	+12.70 (0.04)	+5.59 (0.04)	+5.87 (0.04)	-10.64	-10.53	-3.95	-1.02

Note: Values in parentheses are time (sec) when peak occurs.  
Values for  $F_{ss}$  are taken at 0.5 sec.

negative  $F_{ss}$ 's (or least positive  $F_{ss}$  in the case of C-HB), while the other colored lights are effective to the degree they activate the direct cone input voltages. Thus, positive peaks and  $F_{ss}$ 's arise from different sources.

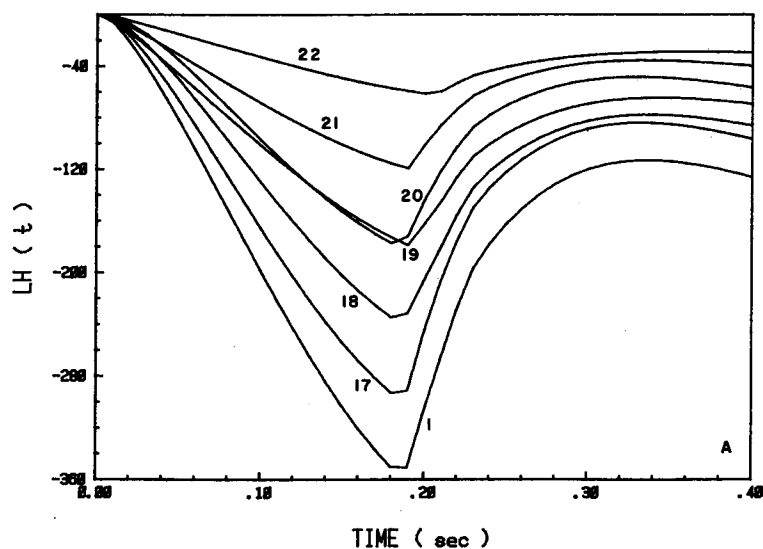


Fig. 5. Effects of elimination of cone-types ( $N_x$ ) on HC(t)'s evoked by white light with  $K_2=0.25$ . A displays effects of elimination of  $N_x$ 's on LH(t)'s in which case  $K_4$  is not involved. B and C display effects of elimination of  $N_x$ 's on CHR(t)'s without (B) and with (C) L-HC input voltage, i.e.  $K_4$ .

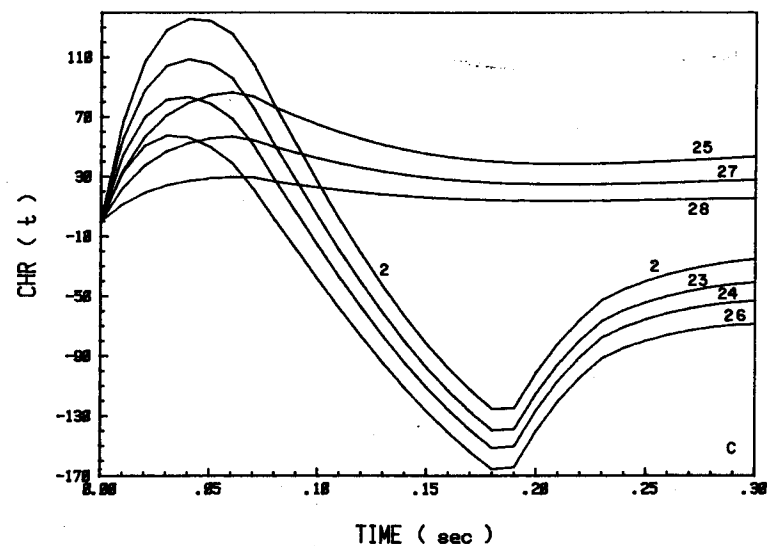
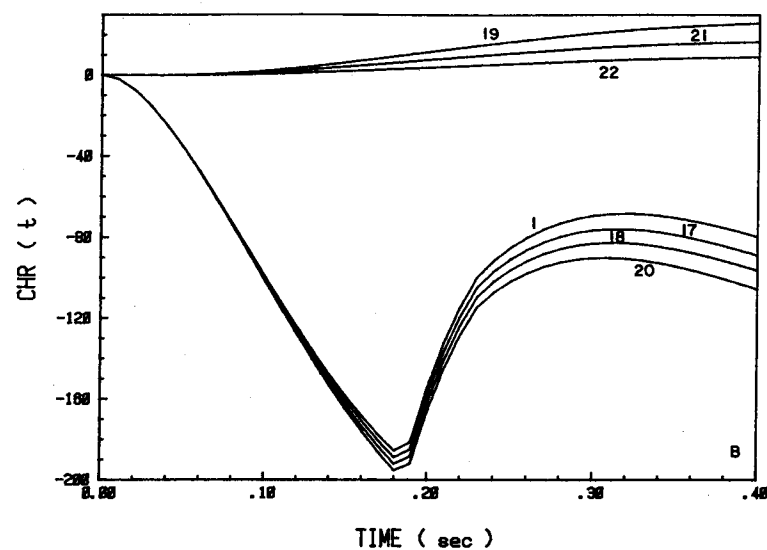


Fig. 5 continued

#### Effects of systematic elimination of cone-types ( $N_x$ ) on HC(t)'s

A LH(t) that is evoked by white light (Fig. 5A) has an initial negative wave that is interrupted at about 0.18 sec by a positive wave peaking at about 0.30 sec and which decays to a steady state level less negative than that existing with  $K_2K_3=0$ . L-HC has

direct input voltages from all 3 cone-types, so that elimination of the blue cone input voltages (i.e.  $N_b=0$ ) has the least effect, while elimination of the red cone direct input voltages (i.e.  $N_r=0$ ) has the greatest effect on  $LH(t)$ . Time course are not radically altered by elimination of  $N_x$ 's (Fig. 5A). For C-HC's (Fig. 5B, C), responses are shown with 2 values of  $K_4$ , (a)  $K_4=0$ , i.e. with no L-HC input voltage to C-HC, and (b)  $K_4=0.25$ , i.e. with the presence of a L-HC input voltage which is antagonistic and with a slower time course than the direct cone input voltage. The results of systematic elimination of  $N_x$ 's are similar for all 4 C-HC's taking into account the relative differences in intensity factors and time constants, so that only  $CHR(t)$ 's are shown. The waveforms of  $CHX(t)$ 's are unaltered (Fig. 5C, D) so long as the direct cone input voltage is present (i.e.  $N_r$  for C-HR,  $N_g$  for C-HG,  $N_b$  for C-HB and  $N_r+N_g$  for C-HY). With  $K_4=0$ , elimination of the direct cone input voltages, eliminates the negative overshoots so that only slow positive waves are seen (Fig. 5B). With  $K_4=0.25$ , the presence of an antagonistic input voltage from L-HC introduces an initial positive peak at about 0.05 sec (Fig. 5C) that is still present, although reduced, if the direct cone input voltages are eliminated. Relative changes are dependent on cone-type dominance, so that the direct red cone input voltages usually have the greatest while the direct blue cone input voltages usually have the least effects.

#### Effects of altering $K_2$ on waveform of $HC(t)$ 's keeping $K_3$ and $K_4$ constant

The initial positive peaks of  $CHX(t)$ 's, which appear at about 0.08 sec when the critical value of  $K_2K_3$  is exceeded, are reduced as  $K_2$  is further increased above the critical level, while the later positive waves of both  $CHX(t)$ 's and  $LH(t)$  become accentuated (Fig. 6A, B). At  $K_2=10$ , all elements including PC's have as waveforms a typical damped sine wave. For  $LH(t)$ , the late positive wave becomes faster and larger as  $K_2$  is increased up to 3, but with higher values of  $K_2$ , the amplitude decreases (Fig. 6A). There is a period from 0 to 0.03 sec where the waveforms are flat and show little change to increasing values of  $K_2$ . For C-HC's (Fig. 6B, C), the initial positive peaks are maximal at the critical level of  $K_2K_3=0.08$  and progressively decrease as  $K_2$  is increased:  $CHB(t)$  is an exception in that a large initial peak appears (Fig. 6C), which corresponds to the appearance of a large positive peak for  $PB(t)$  with  $K_2=10$  (Fig. 1C). The time courses for the positive peak that occurs when  $K_2K_3$  exceeds the critical levels, are the same for all 4  $CHX$ 's, but  $CHY(t)$  peaks the earliest while  $CHB(t)$  peaks the latest (Fig. 6D). Time courses for the later positive wave do not alter significantly.

### 3.3 Bipolar Cells (BC)

#### Introduction

In terms of parameters that can be varied BC's represent a higher order of complexity than HC's or PC's. It is with the BC, with its concentrically oriented antagonistic field, that the basic organization of receptive fields of visual system elements arises. The main parameters to be considered for BC's are those controlling the balance of center and surround field input voltages, i.e.  $K_5$  and  $K_6$  (for C-BC's) or  $K_8$  (for L-BC's).

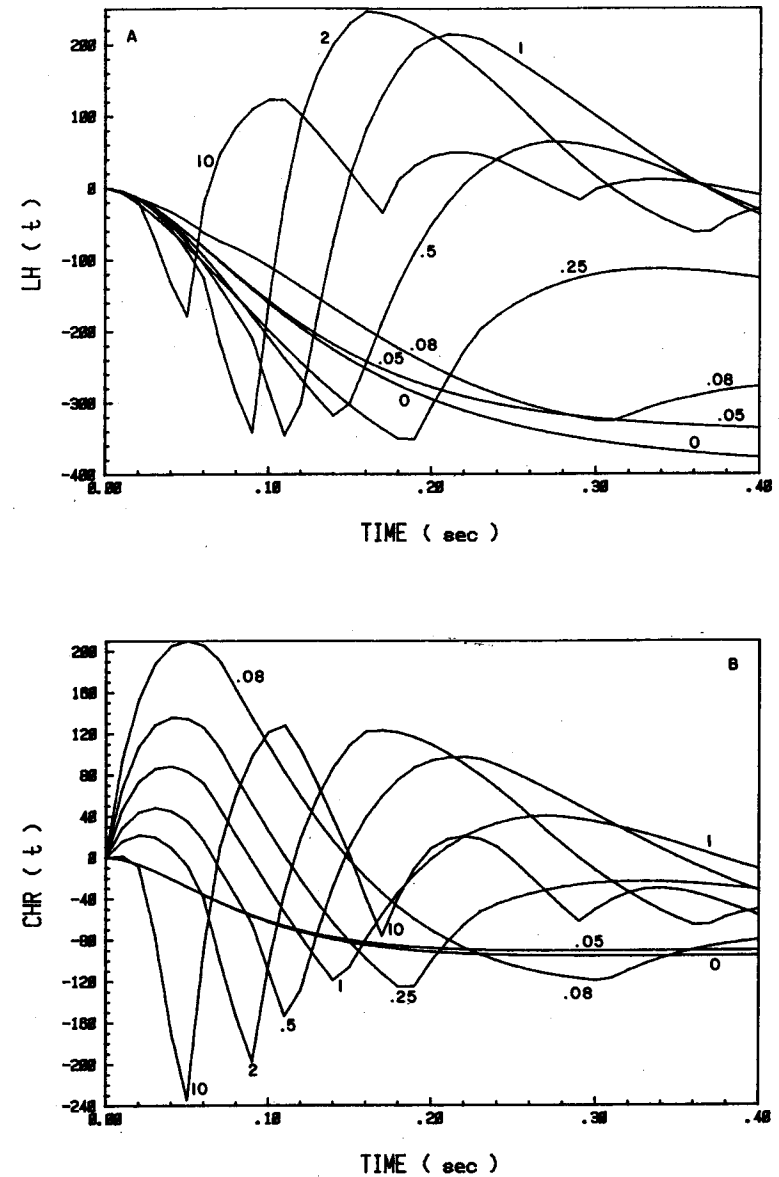


Fig. 6. Effects of negative feedback on waveform of  $CHS(t)$ 's with  $K_3=1$  and  $K_4=0.25$ . A, B and C display effects of varying  $K_2$  on  $LH(t)$ 's,  $CHR(t)$ 's and  $CHB(t)$ 's, respectively. D displays time relationships between  $F(t)$ 's for the 3 cone-types and the 4 HC-types with  $K_2=0.5$ .

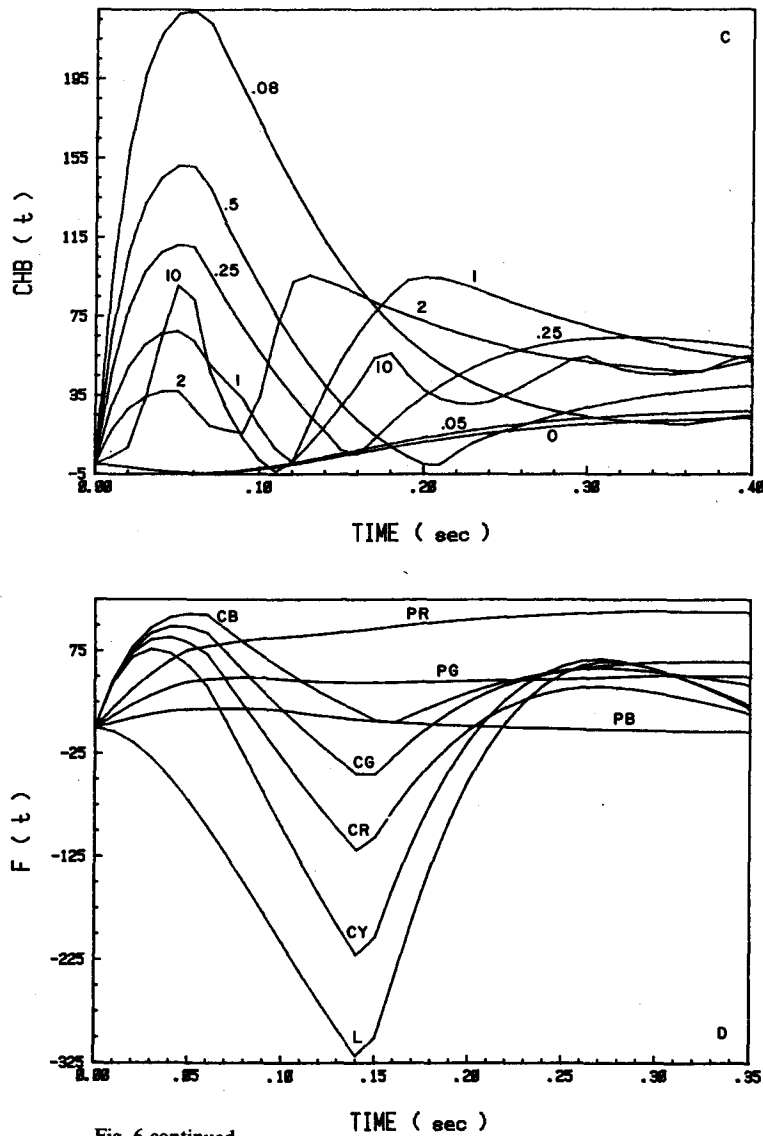


Fig. 6 continued

L-BC's show no color differentiation (Siminoff, 1980a, 1983a, 1984b), while there are 8 color-coded C-BC's, i.e. 4 single-opponents (BPRS, BPGS, BPBS and BPYS) and 4 double-opponents (BPRG, BPGD, BPBD and BPYD). For BPRS as an example of a single-opponent BC, the center field has direct red cone input voltages, so that the surround field is formed by 6 converging C-HG's (which have direct green

cone input voltages); therefore, red cone activation produces the same polarization changes in both center and surround fields. This pattern holds for all of the single opponent C-BC's, i.e. the surround C-HC has as its direct cone input voltage that cone-type which is opponent to the cone-type forming the direct input voltage for the center field. For BPRD as an example of a double-opponent C-BC, the surround field is formed by convergence of 6 C-HR's (which have direct red cone input voltages), so that red cone activation produces opposite polarization changes in center and surround fields. Other double-opponent C-BC's have the same pattern, i.e. the surround-B-HC's have as their direct input voltages that cone-type which also forms the direct input voltages for the center field. Whole field illumination of single-opponent C-BC's by colored lights which maximally activate the cone-type forming the direct input voltage to the center field, will give larger responses than just center field activation alone, since center and surround field responses add. Whole field illumination of double-opponent C-BC's by colored lights, which maximally activate the cone-type having direct input voltages to the center field will give smaller responses than just center field activation alone, since center and surround field responses oppose each other.

#### Effects of balance of center and surround field input voltages on BC(t)'s

##### Center field input voltage only, i.e. $K_6$ or $K_8$ equal to zero

With no negative feedback (i.e.  $K_2=0$ ), the waveform for all BC(t)'s are best described by an exponential curve with positive amplitudes (Fig. 7A). With  $K_2$  below the 1st critical level of 0.052, the waveform of BC(t) is unchanged and only the amplitude is decreased. With  $K_2$  greater than the 2nd critical level of  $K_2K_3=0.0775$ ,

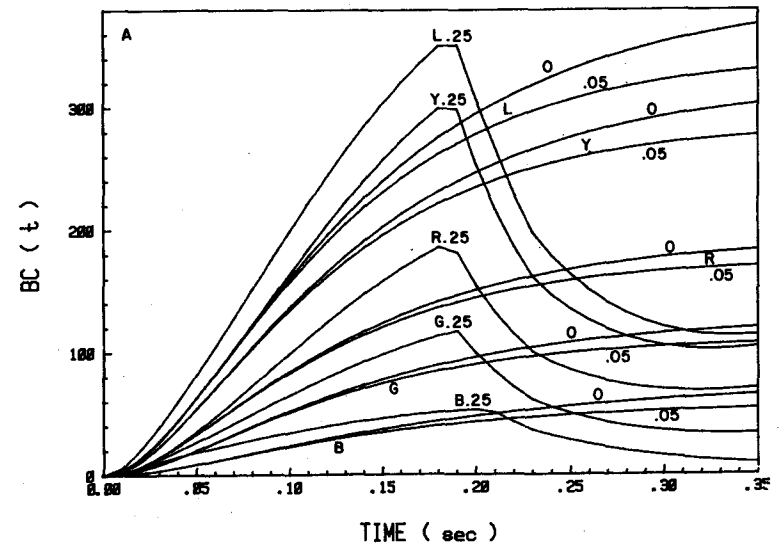


Fig. 7 continued

an initial positive overshoot develops (Fig. 7A) which peaks at about 0.19 sec. Because there is no surround field input voltage present (since  $K_6$  or  $K_8$  is zero), single- and double-opponent C-BC's do not differ in waveform.

*Surround field input voltage only, i.e.  $K_5=0$*

With the presence of a surround field input voltage (i.e.  $K_6$  or  $K_8=1$ ), but in the absence of a center field input voltage (i.e.  $K_5=0$ ) and with  $K_2=0$ , BC(s) show typical exponential waveforms with negative amplitudes (Fig. 7B). With  $K_2=0.05$ , which

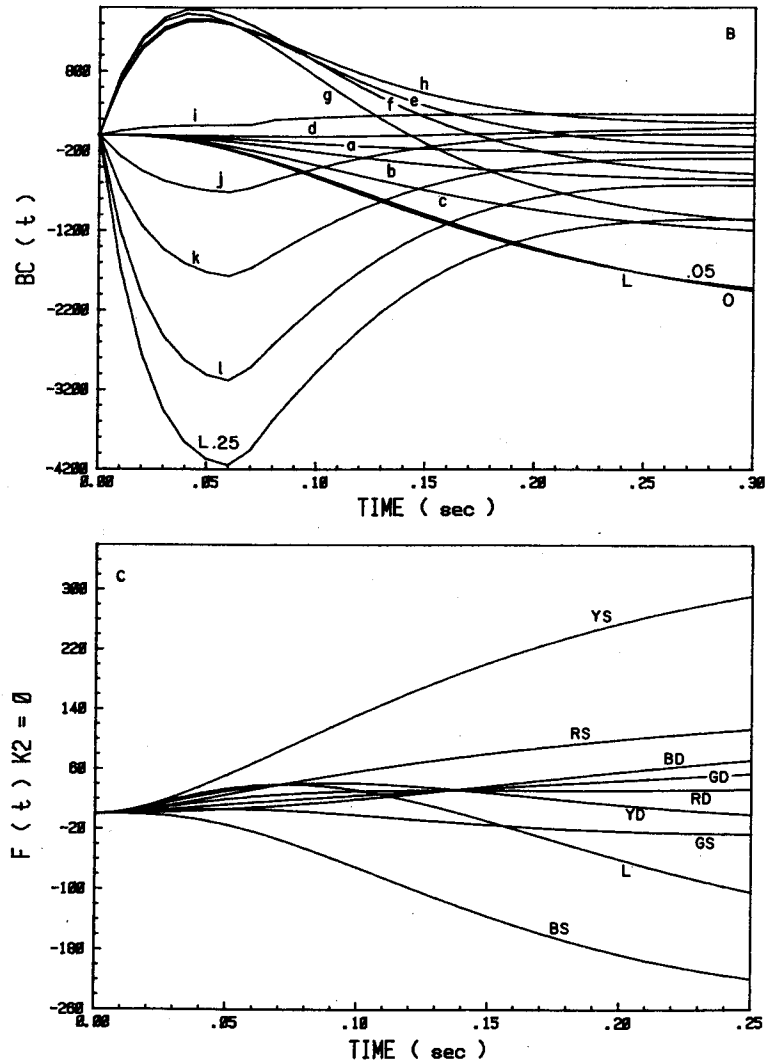


Fig. 7 continued

does not produce damped sine waves, BC(t)'s now display positive overshoots peaking at about 0.06 sec. The initial positive wave is due to negative feedback while the exponential negative wave is due to the presence of a surround field input voltage. For  $K_2=0.25$ , the positive peaks are now replaced by extremely large negative overshoots that peak at about 0.07 sec and arise from the direct cone input voltages.

*Mixing of center and surround field input voltages*

BC(t)'s with mixed center and surround field input voltages are the resultant of 2 antagonistic input voltages with differing time courses.  $F_{ss}$ 's will depend on which input voltage dominates and whether one is considering a single- or a double-opponent C-BC. With  $K_2=0$  and with red cones representing the dominant input voltage, BPRS(t) and BPYS(t), where red cones give direct input voltages, show positive exponential waveforms, but BPGS(t) and BPBS(t), where red cones

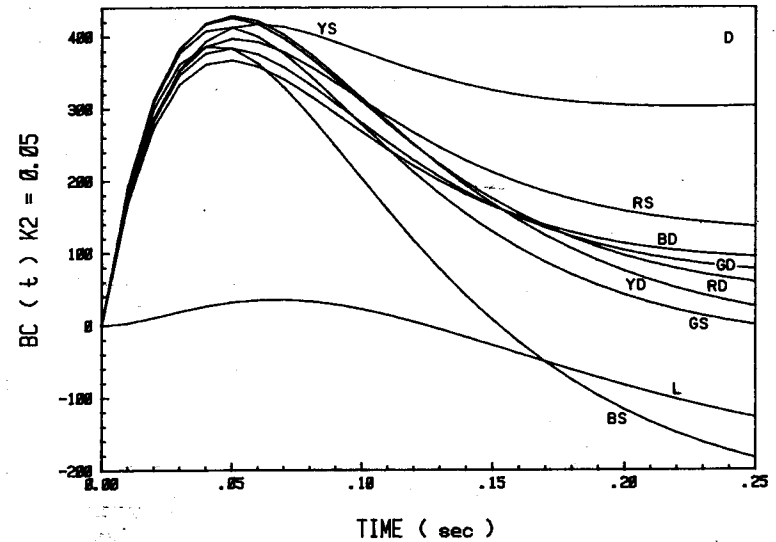
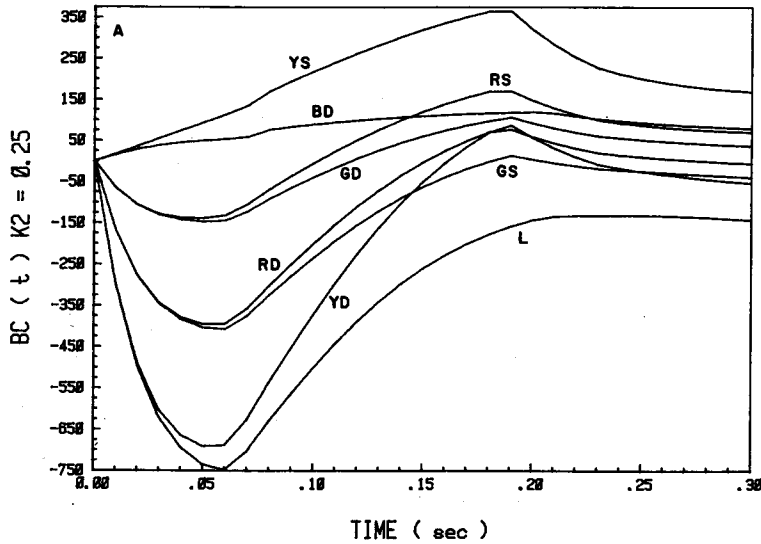


Fig. 7. Generated output voltages for BC's evoked by white light. A displays BC(t)'s evoked with no surround field input voltages (i.e.  $K_6$  or  $K_8=0$ ) and  $K_5=1$ ,  $K_3=1$  and  $K_4=0$ . Single- and double-opponent C-BC's give identical curves since there are no surround field input voltages so  $L=L$ -BC, and  $R$ ,  $G$ ,  $B$  and  $Y$  refer to their respective BPXS or BPXD. For each BC, there are 3 curves representing  $K_2=0$ , or 0.05 or 0.25. B, same as for A except that now there are no center field input voltages (i.e.  $K_5=0$ ) and  $K_6$  or  $K_8=1$  with  $K_3=1$  and  $K_4=0.25$ .  $L=L$ -BC;  $a, h, l=B$ PYD or  $B$ S;  $b, e, k=B$ PRD or  $G$ S;  $c, f, j=B$ PGD or  $R$ S;  $d, g, i=B$ PBD or  $Y$ S. Three letters of each group of C-BC's refer to  $K_2=0$ , 0.25 and 0.25, respectively. Note that without a center field input voltage, single-opponent C-BC has same  $F(t)$  as double-opponent C-BC of its antagonist in color pair. C and D display BC(t)'s with mixed center and surround field input voltages with  $K_2=0$ (C) and  $K_2=0.25$ (D) and  $K_3=1$ ,  $K_4=0.25$ ,  $K_5=1$  and  $K_6$  or  $K_8=0.25$ . Letters refer to type of single-(S) or double-(D) opponent C-BC.

dominate via an antagonistic surround field input voltage, show negative exponential waveforms. For both BPRD and BPYD, the initial positive exponential waveform is replaced by a slower negative exponential wave arising from the antagonistic surround field, while for BPGD and BPBD the initial negative exponential wave is reinforced by a surround field input voltage. L-BC acts like C-BY since they differ only by the presence of a weak blue cone input voltage in L-BC. BC(t)'s resulting from mixed center and surround field input voltages (Figs. 7D, 8A) are similarly explained as the linear summation of 2 antagonistic input voltages, but now, each is modified by negative feedback with red cone dominance play an important role.

*Effects of colored lights on evoking BC(t)'s*

Waveforms of BC's evoked by colored and white lights are similar with only the amplitudes changing. Table 3 tabulates the effectiveness of various colored lights with  $K_2=0.25$  to evoke the initial negative peak, the secondary peak and the amplitude of the dc level ( $F_{ss}$ ) as illustrated in Fig. 8A. Yellow and red colored lights are more effective than green and blue colored lights in evoking the initial negative wave (Table 3). BPBD and BPYS are exceptions in that yellow and red colored lights do not evoke negative overshoots, while green and blue colored lights evoke small negative waves that are quickly replaced by positive waves. The secondary positive peak and  $F_{ss}$  are for the most part more effectively generated by either yellow or red colored lights than by green or blue colored lights; the only exception is BPBS for



**Fig. 8.** Generated output voltages for BC's with  $K_2=0.25$ . A, same as in Fig. 7C,D except that now  $K_2=0.25$ . B, C and D display effects of elimination of cone-types ( $N_2$ ) on  $F(t)$ 's for L-BC (B), BPRS (C) and BPRD (D) evoked by white light and  $K_2=0.25$ .

**Table 3.** Relative effectiveness of colored lights to evoke BC(t)'s.

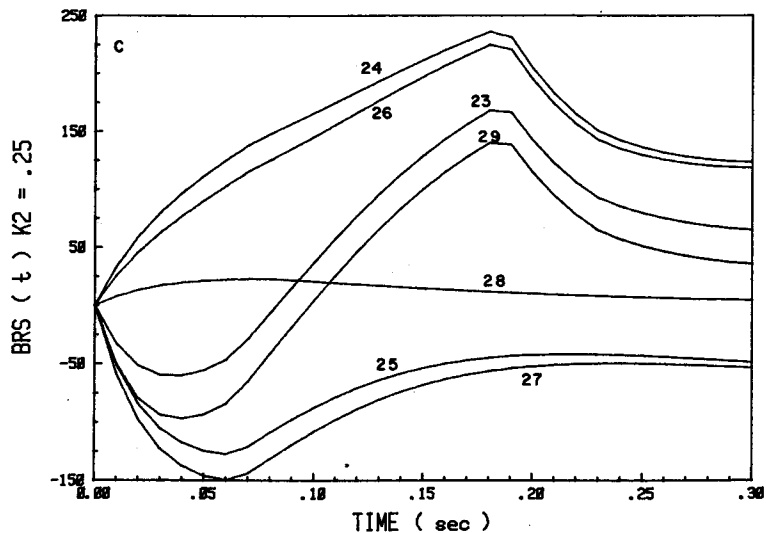
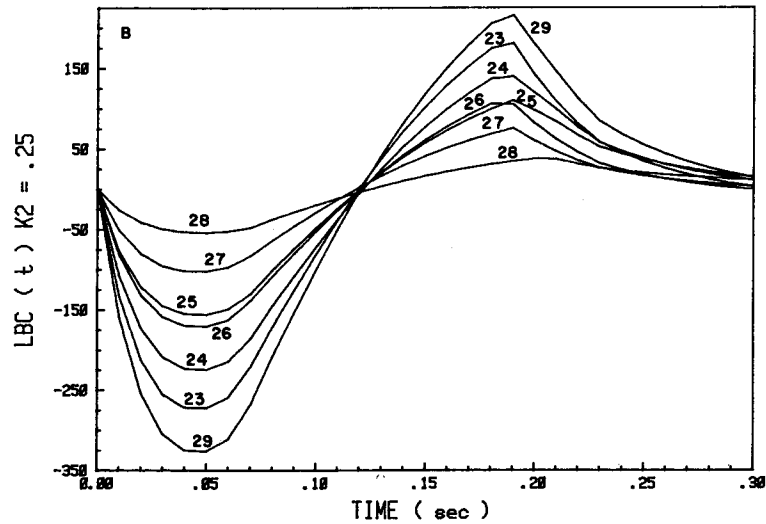
BC(t)	Initial Negative peak				Positive peak				$F_{ss}$			
	YL	RL	GL	BL	YL	RL	GL	BL	YL	RL	GL	BL
LBC	-36.6 (0.05)	-35.7 (0.05)	-15.4 (0.05)	-16.2 (0.05)	+24.4 (0.19)	+23.7 (0.19)	+10.4 (0.19)	+10.9 (0.19)	+4.5 (0.19)	+4.4 (0.19)	+2.0 (0.19)	+2.1 (0.19)
BPRS	-7.3 (0.04)	-5.7 (0.03)	-4.8 (0.04)	-4.3 (0.04)	+16.3 (0.18)	+17.7 (0.18)	+4.6 (0.18)	+5.5 (0.18)	+7.6 (0.18)	+9.0 (0.18)	+1.2 (0.18)	+2.0 (0.18)
BPRD	-11.7 (0.04)	-13.0 (0.04)	-2.6 (0.04)	-3.3 (0.04)	+14.6 (0.18)	+14.7 (0.18)	+5.5 (0.18)	+6.0 (0.18)	+6.2 (0.18)	+6.3 (0.18)	+2.2 (0.18)	+2.4 (0.18)
BPGS	-11.6 (0.05)	-13.4 (0.05)	-2.2 (0.03)	-2.9 (0.04)	+12.3 (0.19)	+10.1 (0.19)	+7.5 (0.19)	+7.1 (0.19)	+4.1 (0.19)	+2.4 (0.19)	+3.6 (0.19)	+3.1 (0.19)
BPGD	-7.2 (0.04)	-5.8 (0.04)	-4.3 (0.04)	-3.9 (0.04)	+13.9 (0.19)	+12.9 (0.19)	+6.5 (0.19)	+6.6 (0.19)	+5.6 (0.19)	+5.1 (0.19)	+2.7 (0.19)	+2.7 (0.19)
BPBS	-30.2 (0.06)	-30.0 (0.06)	-11.4 (0.06)	-12.0 (0.06)	-1.0 (0.21)	-1.4 (0.21)	+0.8 (0.21)	+0.9 (0.21)	-6.5 (0.21)	-6.7 (0.21)	-1.7 (0.21)	-1.7 (0.21)
BPBD	-	-	-0.2 (0.01)	-0.3 (0.01)	+9.6 (0.20)	+9.1 (0.20)	+4.5 (0.20)	+4.7 (0.20)	+4.2 (0.20)	+4.0 (0.20)	+2.0 (0.20)	+2.1 (0.20)
BPYS	-	-	-0.1 (0.01)	-0.2 (0.01)	+35.3 (0.19)	+34.6 (0.19)	+14.0 (0.19)	+14.6 (0.19)	+18.6 (0.19)	+18.4 (0.19)	+6.9 (0.19)	+7.2 (0.19)
BPYD	-25.5 (0.04)	-25.2 (0.04)	-9.8 (0.04)	-10.3 (0.04)	+23.9 (0.19)	+23.3 (0.19)	+10.0 (0.19)	+10.4 (0.19)	+7.9 (0.19)	+7.7 (0.19)	+3.2 (0.19)	+3.3 (0.19)

Note: Values in parentheses are time (sec) when peak occurs. Values for  $F_{ss}$  are taken at 0.5 sec.

which the secondary positive peak and  $F_{ss}$  are more effectively generated by green or blue colored lights.

*Effects of systematic elimination of cone-types ( $N_x$ ) on  $BC(t)$ 's*

Three portions of each curve can be considered, the initial negative peak, the late positive peak and  $F_{ss}$ . For L-BC, which represents the BC with the simplest organization, the results are straightforward (Fig. 8B). A combination of all 3



cone-types as input is most effective in generating all 3 parameters, while blue cones alone are the least effective (Table 4). In general, the order of effectiveness is the same as the order of numbers of cones, i.e. red > green > blue. For single-opponent C-BC's (Fig. 8C, D), the least effective stimulus for evoking the initial negative peak is the

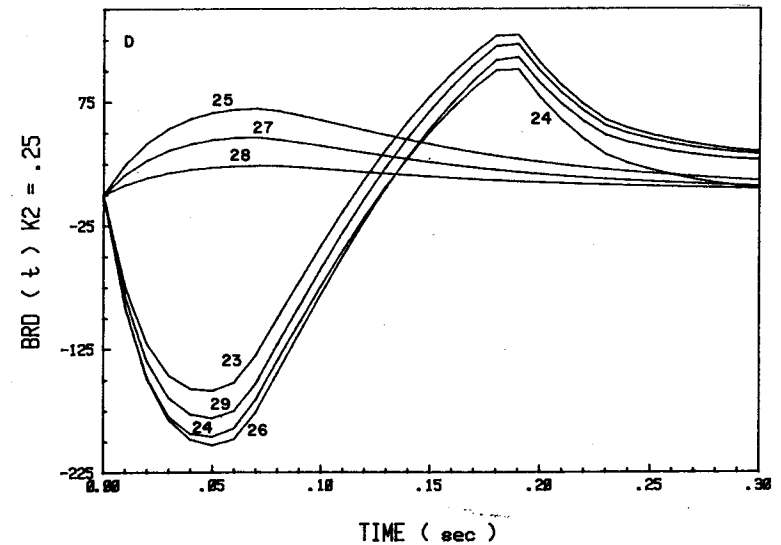


Fig. 8 continued

absence of an input voltage from the 2nd color of the opponent color pair (i.e. green for BPRS, red for BPGS, red+green for BPBS and blue for BPYS), while for double-opponent C-BC's (Table 4), the absence of the direct cone-type is the least effective stimulus (i.e. red for BPRD, etc). The initial portion of the curve is positive for single-opponent C-BC's when the input voltage from the 2nd color of the color pair is missing, and for double-opponent C-BC's when the direct cone input voltage is absent (Fig. 8C, D). As a corollary, the most effective stimuli to evoke the initial negative peaks of single- and double-opponent C-BC's are the absence of input voltages from the 2nd color of the color pair and the direct color, respectively. For the late positive peak, the presence of input voltages from the direct cone-type is the least effective stimulus, while input voltages from cones of the 2nd color of the color pair are more effective as stimuli: these results are opposite to those obtained on the initial negative peak with cone-type elimination. In general, the same order of effectiveness is followed in generating  $F_{ss}$  as for inducing the positive peak, but with some variability (Table 4).

*Effects of negative feedback ( $K_2$ ) on  $BC(t)$ 's*

The maximum amplitude for the initial negative peak occurs when  $K_2$  just exceeds the 2nd critical level (i.e.  $K_2K_3=0.08$ ) and the amplitude rapidly decreases with

Table 4. Effects of elimination of cones ( $N_x$ ) on  $BC(t)$ 's using white light.

IC	F(t)	1	2	3	4	5	6	7
'A	A	-326.1(0.05)	+272.2(0.05)	-224.3(0.05)	-155.7(0.05)	-170.4(0.05)	-101.8(0.05)	-53.9(0.05)
	B	+215.7(0.19)	+181.0(0.19)	+140.0(0.19)	+110.2(0.19)	+106.1(0.18)	+75.6(0.19)	+37.8(0.20)
	C	+39.1	+28.9	+26.9	+22.4	+16.7	+12.2	+10.2
'RS	A	-97.0(0.04)	-59.9(0.04)	-	-127.15(0.06)	-	-149.5(0.06)	-
	B	+139.8(0.18)	+167.8(0.18)	+235.8(0.18)	-42.1(0.22)	+224.4(0.18)	-49.9(0.24)	+22.7(0.07)
	C	+63.0	+94.3	+164.5	-65.6	+162.1	-67.9	+2.3
'RD	A	-196.1(0.05)	-158.7(0.05)	-181.0(0.05)	-	-203.0(0.05)	-	-
	B	+101.2(0.19)	+128.9(0.19)	+121.4(0.19)	+69.5(0.07)	+110.8(0.19)	+46.2(0.07)	+23.3(0.07)
	C	+26.9	+58.2	+57.1	+5.7	+54.8	+3.4	+2.3
'GS	A	-204.6(0.05)	-172.8(0.05)	-211.6(0.05)	-	-246.5(0.06)	-	-
	B	+37.1(0.19)	+63.7(0.19)	-72.8(0.24)	+167.3(0.19)	-80.1(0.26)	+155.4(0.19)	+29.0(0.07)
	C	-24.9	+6.4	-99.9	+111.0	-102.3	+108.7	+2.4
'GD	A	-101.8(0.05)	-69.7(0.04)	-	-97.1(0.04)	-	-123.8(0.05)	-
	B	+74.5(0.19)	+101.0(0.19)	+82.8(0.06)	+95.0(0.19)	+54.7(0.06)	+83.0(0.19)	+28.4(0.07)
	C	+11.2	+42.4	+7.4	+39.8	+5.0	+37.4	2.4
'BS	A	-345.7(0.06)	-331.8(0.06)	-167.8(0.06)	-74.6(0.05)	-213.8(0.06)	-118.0(0.06)	-
	B	-60.5(0.21)	-105.2(0.25)	+16.0(0.20)	+46.9(0.20)	-65.5(0.26)	-39.1(0.23)	+87.2(0.20)
	C	-104.4	-143.2	-13.7	+15.4	-86.2	-57.0	+72.5
'BD	A	-29.5(0.04)	-	-17.8(0.04)	-20.2(0.03)	-	-	-64.8(0.06)
	B	+42.0(0.20)	+99.7(0.06)	+60.1(0.20)	+61.5(0.20)	48.9(0.06)	+51.3(0.07)	+42.0(0.20)
	C	+0.9	+9.9	+30.4	+28.7	+5.8	+4.1	+24.6
'YS	A	-17.8(0.02)	-	-5.9(0.01)	-18.3(0.02)	-	-	-72.5(0.07)
	B	+286.4(0.19)	+358.9(0.18)	+180.9(0.18)	+115.2(0.19)	+214.6(0.18)	+148.2(0.19)	-32.7(0.21)
	C	+143.4	+226.6	+86.0	+41.5	+135.5	+91.0	-49.5
'YD	A	-298.0(0.05)	-275.3(0.05)	-135.6(0.04)	-69.0(0.04)	-172.0(0.05)	-103.3(0.05)	-
	B	+175.5(0.19)	+200.0(0.19)	+129.3(0.18)	+99.4(0.19)	+114.5(0.19)	+85.5(0.19)	+38.8(0.07)
	C	+38.1	+73.4	+41.8	+28.2	+43.5	+29.9	-1.7

IC: A = initial negative peak; B = positive peak; C =  $F_{sr}$ .  
 Values in parenthesis are time (sec) when peak occurs.  
 For columns, 1-NR,NG, and NB have maximum values; 2-NB=0; 3-NG=0; 4-NR=0; 6-NR,NB=0; 7-NR,NG=0

further increases of  $K_2$  (Fig. 9A-D). The late positive peak first appears at about  $K_2=0.25$ , reaches its maximum amplitude at  $K_2=2$  and then decreases with increasing  $K_2$ . The typical damped sine wave first appears at higher values of  $K_2$ .

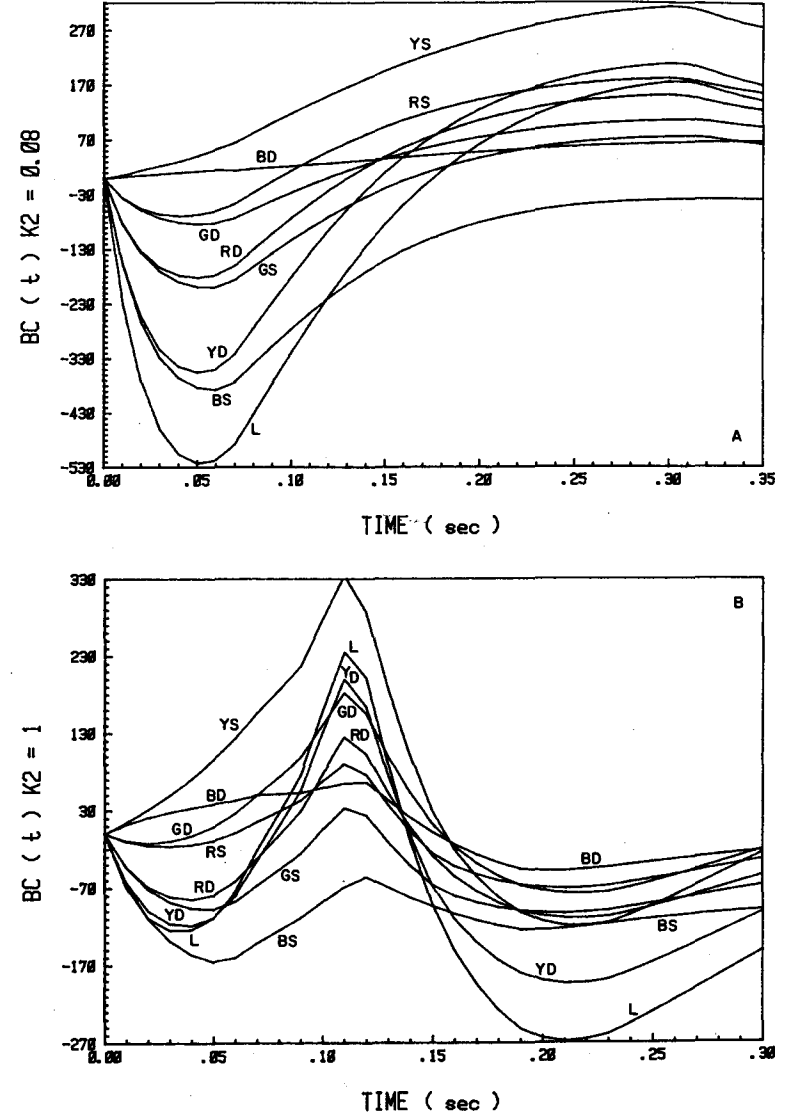


Fig. 9. Effects of negative feedback on waveforms of  $BC(t)$ 's evoked by white light. Parameters are  $K_3=1$ ,  $K_4=0.25$ ,  $K_5=1$  and  $K_6$  or  $K_8=1$ . Negative feedback (i.e.  $K_2K_3$ ) is varied by altering  $K_2$  to

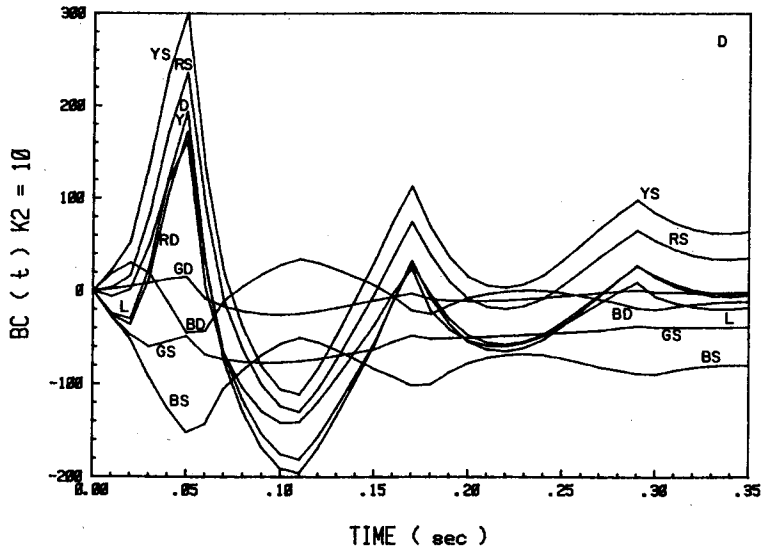
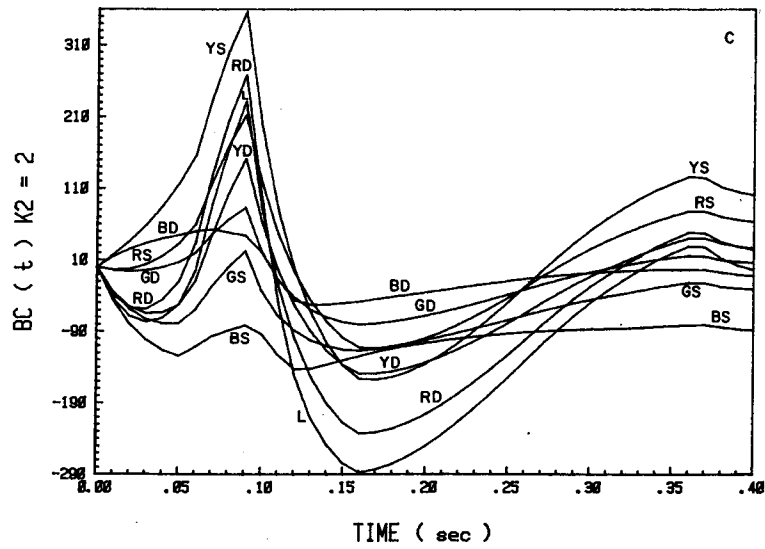


Fig. 9 continued

3.4 Steady State Levels ( $F_{ss}$ )

Equations for  $F_{ss}$ 's are derived by using only the non-time-dependent terms of the mathematical expressions (see Table 10 of Part A).

Cone pedicles

PC's have 2 gain factors that can be varied,  $K_2$  and  $K_3$ , each of which is involved with controlling negative feedback.  $F_{ss}$  decreases with increasing values of  $K_2$  (Fig. 10A) or  $K_3$  (Fig. 10B). In Fig. 10A, the dotted lines connect points on the curves

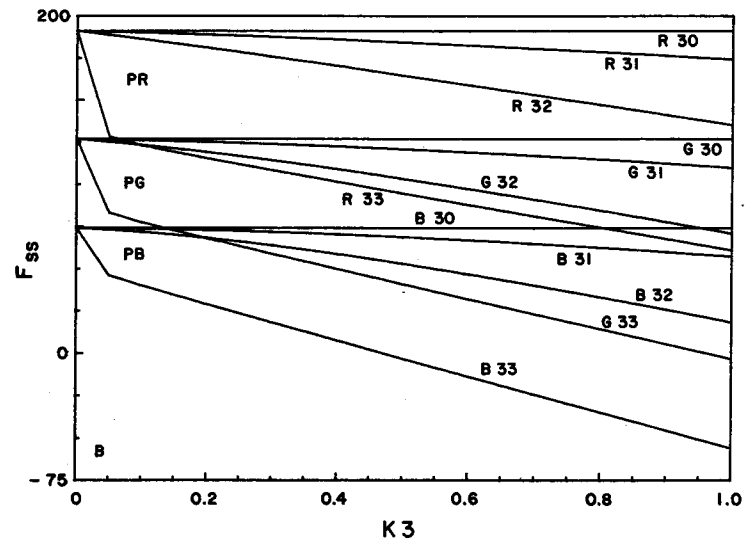
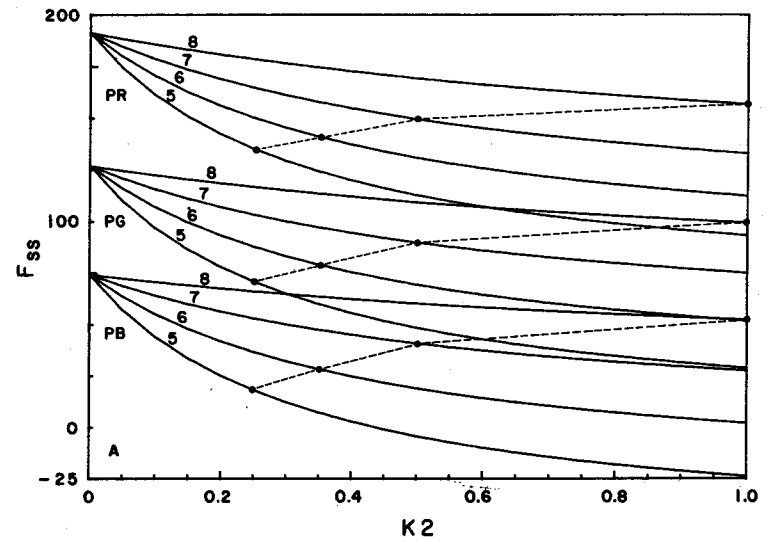


Fig. 10. Steady state values ( $F_{ss}$ ) for generated output voltages of PC's evoked by white light. A displays effects of increasing  $K_2$  (x-axis) on  $PX(t)$ 's with 4 indicated values of  $K_3$ . B displays effects of increasing  $K_3$  (x-axis) on  $PX(t)$ 's with 4 indicated values of  $K_2$ .

for  $PC(t)$  having the common value of  $K_2K_3 = 0.25$  ( $K_3$  is constant while  $K_2$  changes). If only negative feedback via the direct cone input voltage were involved, then these dotted lines should form a family of straight lines. Deviations from a straight line at the higher values of  $K_2$  represent the contributions of negative feedback loops from other cone-types which do not have direct input voltages. With very high values of  $K_2$ , there are sharp breaks in all 3 curves at about  $K_3 = 0.05$  (Fig. 10B), which are equivalent to  $K_2K_3 = 5.0$  and  $K_2K_3^2 = 0.25$ , reflecting the dual effects of  $K_3$  (see equation for  $PX\{t\}$  in Table 10 of Part A). With  $K_2 = 100$ , zero crossings occur at  $K_3 = 1.8, 0.93$  and  $0.47$  for  $PR(t)$ ,  $PG(t)$  and  $PB(t)$ , respectively.

### Horizontal cells

HC's have 3 gain factors to be considered,  $K_2$  and  $K_3$  as with the PC's, and  $K_4$  which control the amount of antagonistic input voltages from L-HC to C-BC. The family of plots of  $F_{ss}-K_2$  (Fig. 11A) is typical for all C-HC's with only absolute levels varying.

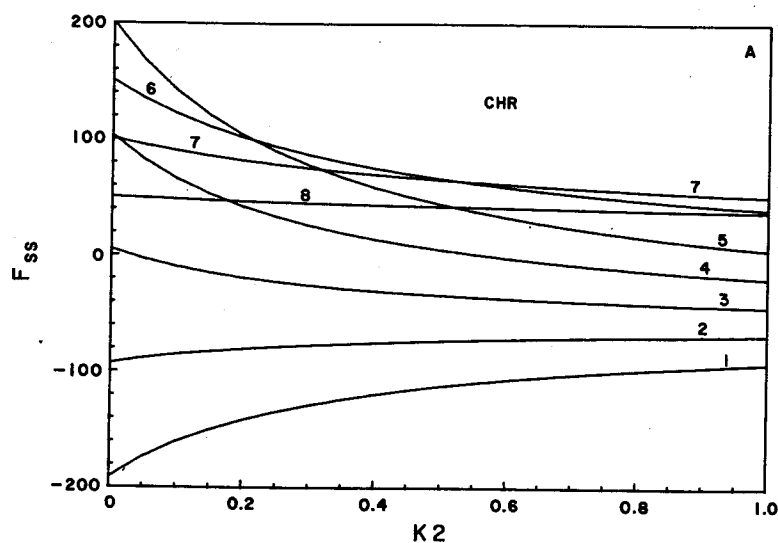


Fig. 11. Steady state values of generated output voltages of HC's evoked by white light. A displays effects of altering  $K_2$  (x-axis) on  $F_{ss}$ 's of C-HR with 2 sets of curves,  $K_3$  is kept constant (1-5) and  $K_4$  is kept constant (6-8). B displays effects of altering  $K_3$  or  $K_4$  on  $F_{ss}$ 's of 4 types HC's with  $K_2 = 0$ . Either  $K_3$  is kept constant and  $K_4$  is varied (34) or else  $K_4$  is kept constant and  $K_3$  is varied (30). x-axis ( $K_2$ ) refers to either  $K_3$  or  $K_4$ , depending on which is being varied. C displays effects of altering  $K_2$  on  $F_{ss}$ 's of L-HC; otherwise same as A. D is same as B except  $K_2 = 100$ .

Table 5. Zero crossings of  $K_4$  axis for  $CHX(t)$ 's.

CHX	CHX(t) when $K_2K_3$ is:			
	0	0.05	0.25	100
CHR	0.50	0.52	0.62	—
CHG	0.35	0.35	0.35	—
CHB	0.26	0.20	0.10	0-1
CHY	0.82	0.85	0.94	—

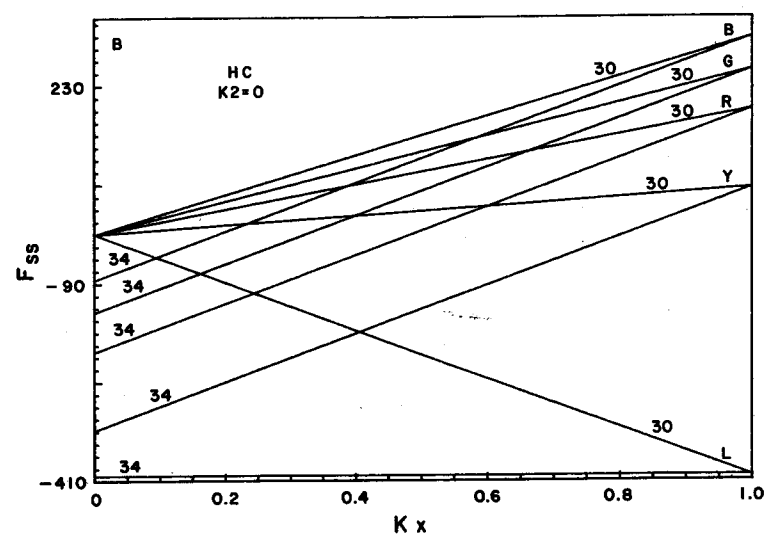


Fig. 11 continued

$F_{ss}$  increases (i.e. becomes less negative or more positive) with increasing values of  $K_2$  when the initial value is less than the final value to which the curve asymptotes (i.e.  $K_2 = 100$ ), and decreases (i.e. becomes more negative or less positive) when the initial value is greater than the final value. Plots of  $F_{ss}-K_4$  form families of parallel straight lines with  $K_3 = 1$  and  $K_2 = 0$  (Fig. 10B). All 4 C-HC's have negative  $F_{ss}$ 's when  $K_2 = 0$  and  $K_3 = 1$  and have zero crossings at  $K_4 = 0.5, 0.35, 0.20$  and  $0.82$  for C-HR, C-HG, C-HB and C-HY, respectively (Table 5). At  $K_2 = 100$ ,  $F_{ss}$ 's are always negative for L-HC, C-HR and C-HY and always positive for C-HG and C-HB. When  $K_4$  is kept constant at 1.0, all 4 C-HC's have positive  $F_{ss}$ 's at the maximum value of  $K_3 = 1$  and decrease as  $K_4$  decreases (Fig. 11B) with zero crossings occurring at  $K_3 = 0$  for all 4 C-HC's. Slopes of the  $F_{ss}$  curves obtained by varying either  $K_3$  or  $K_4$  depend on the value for  $K_2$  (Fig. 11A) and decrease with increasing values of  $K_2$ . For L-HC,  $F_{ss}$  is not

affected by changing  $K_4$ , but is affected by changes in  $K_2K_3$  (Fig. 11C).  $F_{ss}$ 's increase (i.e. become less negative) with increasing values of  $K_2$  or decreasing values of  $K_3$ , but decrease as  $K_3$  increases reflecting the dual effects of  $K_2K_3$  and  $K_2K_3^2$  on the direct and indirect input voltages. With  $K_2=100$ ,  $F_{ss}$ 's do not change when  $K_3=1$  and  $K_4$  is increased (Fig. 11D). With  $K_3$  changing from 1.0 to 0.25 while keeping  $K_4=1$  and  $K_2=100$ ,  $F_{ss}$ 's of C-HC's initially increase and then decrease as  $K_3$  further increases; for L-HC,  $F_{ss}$ 's are increased and then decreased (Fig. 11D).

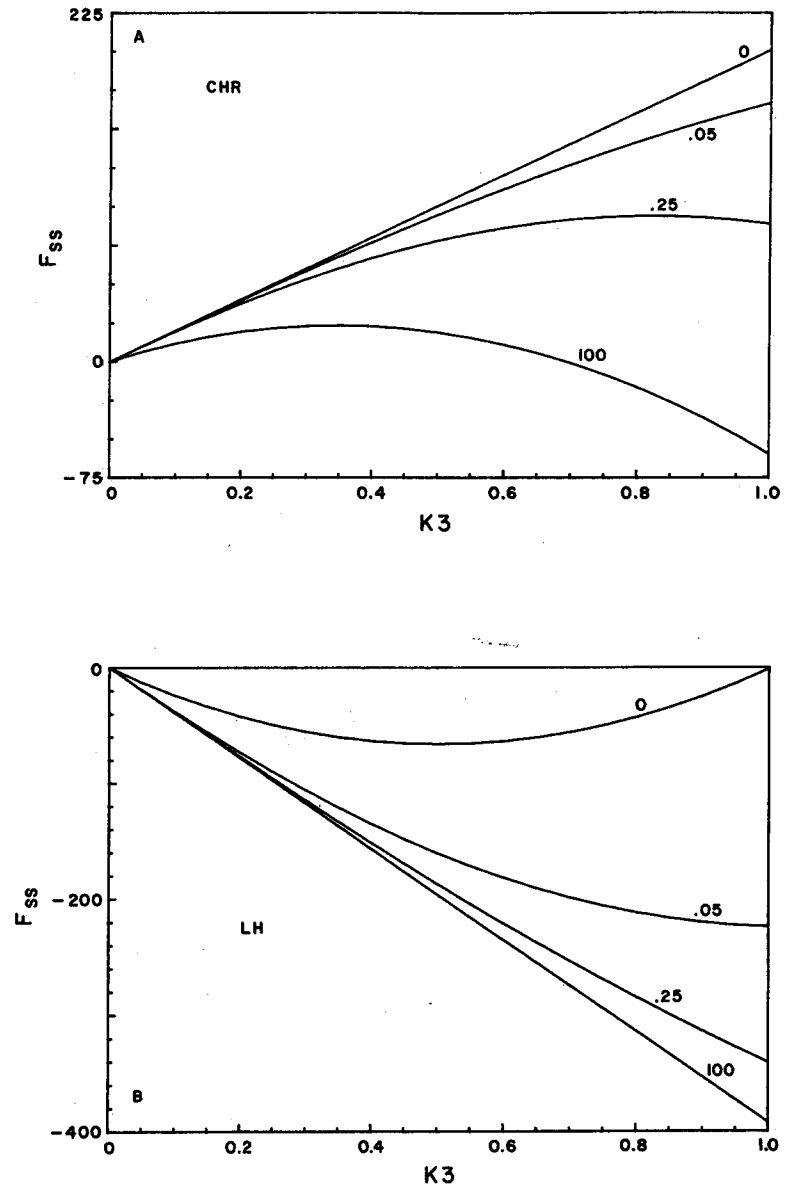
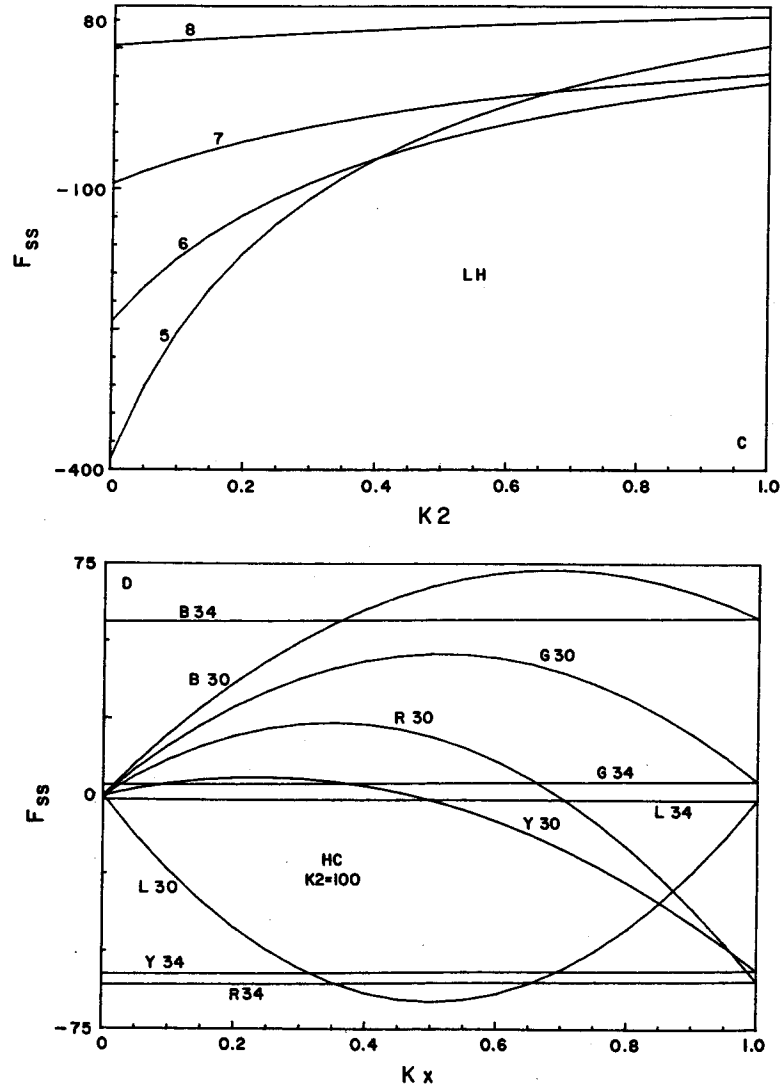


Fig. 12. Steady state values of generated voltages for HC's evoked by white light. A displays effects of increasing  $K_3$  (x-axis) on  $F_{ss}$ 's of C-HR with  $K_4=1$ . Numbers designating curves refer to values of  $K_2$ . B is same as A except for L-HC. C displays effects of increasing  $K_4$  (x-axis) on  $F_{ss}$ 's of C-HR with  $K_3=1$ . Values of  $K_2$  are indicated as before.

When  $K_2=0$ ,  $F_{ss}$ 's of C-HR (and other C-HC's) increase linearly as  $K_3$  increases (Fig. 12A). With increasing values of  $K_2$ , the curves deviate further and further from linearity such that at  $K_2=100$  there is an initial slight increase, after which the curve shows a marked decrease.  $F_{ss}$ 's for L-HC and C-HX are mirror images (Fig. 12B).

Fig. 12C depicts the effects of increasing  $K_4$  while keeping  $K_3$  constant and using 4 values for  $K_3$ , i.e. 0, 0.05, 0.25 and 100. Only the curves for C-HR are shown, but the other C-HC's behave in a similar manner. With  $K_4=0$ , the maximum and minimum negative values for  $F_{ss}$  of a C-HC occurs at  $K_2=0$  and  $K_2=100$ , respectively. With  $K_4=1$ , the order is reversed and  $K_2=0$  and 100 have the maximum and minimum positive values, respectively. All 4 curves are linear with slopes decreasing to nearly

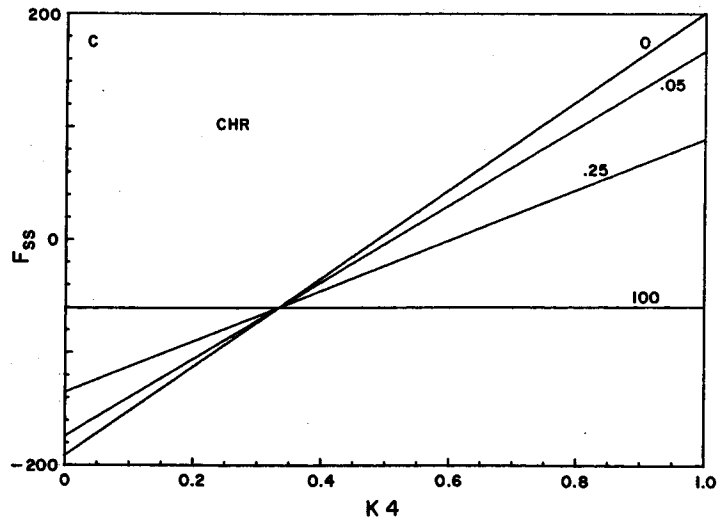


Fig. 12 continued

zero from its maximum at  $K_2=0$  to its minimum at  $K_2=100$ .  $K_4=0.35$  represents an isoelectric point and zero crossings are the same for C-HR, C-HG and C-HB, while C-HY has an isoelectric point at 0.67. Crossover values follow those of their cone-type input voltages (Table 5), C-HY, with R+G, has the largest value of  $K_3$ , while C-HB, with only a blue cone input voltage, has the smallest value. C-HG has all 3 crossover values at the isoelectric point  $K_4=0.35$ .

#### Bipolar cells

With no surround field input voltage (i.e.  $K_6$  or  $K_8=0$ ),  $F_{ss}$ 's are positive with  $K_2=0$  and decrease with increasing values of  $K_2$  (Fig. 13A). Since  $K_6=0$ , single- and double-opponent C-BC's give identical  $F(t)$ 's. With no center field input voltages (i.e.  $K_5=0$ ),  $F_{ss}$ 's are negative with  $K_2=0$  and increase (i.e. decrease in negativity) with

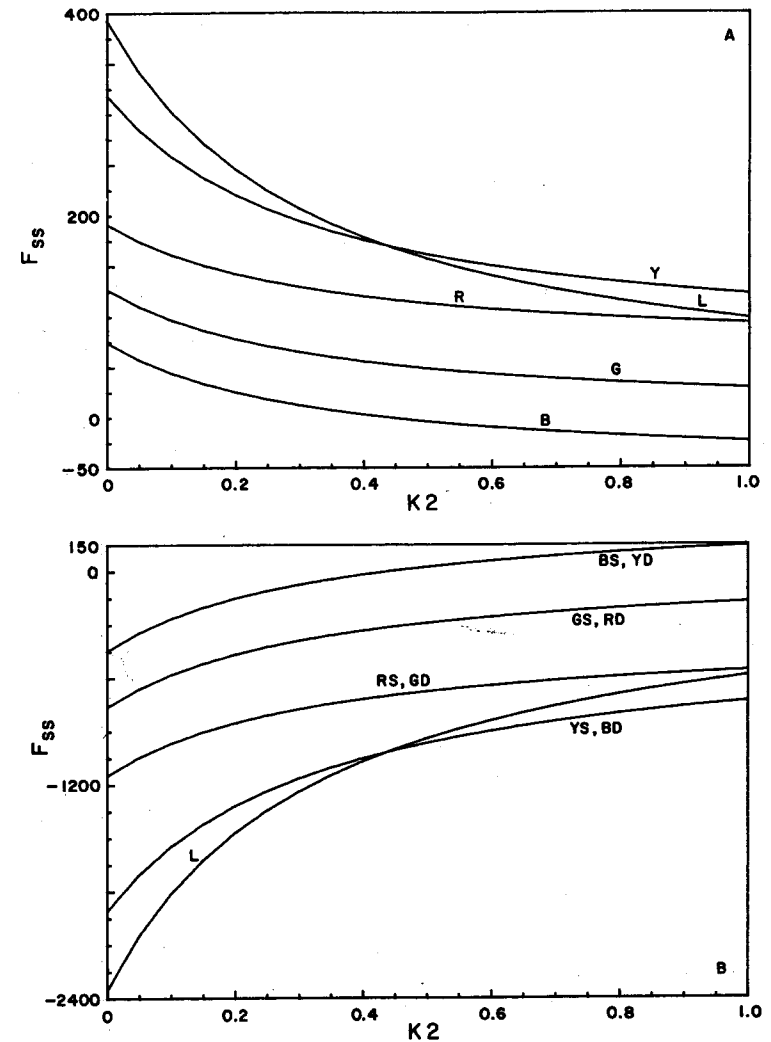


Fig. 13. Steady state values of generated voltages of BC's evoked by white light. A displays effects of increasing  $K_2$  (x-axis on  $F_{ss}$ 's of BC's with no surround field input voltages, i.e.  $K_6$  or  $K_8=0$  and  $K_3=1$ ,  $K_4=0$  and  $K_5=1$ . Since there are no surround field input voltages, single- and double-opponent  $F(t)$ 's are identical for C-BC's. L, R, G, B and Y designate BC-types. B displays effects of increasing  $K_2$  (x-axis) on  $F_{ss}$ 's of BC's with no center field input voltages, i.e.  $K_5=0$  and  $K_3=1$ ,  $K_4=0$  and  $K_6$  or  $K_8=1$ . Since there are no center field input voltages,  $F(t)$  of single-opponent of C-BC of one color is identical to double-opponent of C-BC of its antagonistic color. C displays effects of varying surround field input voltage, i.e.  $K_6$  or  $K_8$  (x-axis) on  $F_{ss}$ 's on BC's with  $K_2=0.25$ ,  $K_3=1$ ,  $K_4=0$  and  $K_5=1$ . D is same as C except L-HC input voltages to C-HC's are present, i.e.  $K_4=1$ .

increasing values  $K_2$  (Fig. 13B). When the center and surround field input voltages are mixed, intermediate curves are observed that are the linear addition of 2 antagonistic inputs. For each  $BC(t)$ , there is a combination of values of  $K_i$ 's that gives  $F_{ss}=0$  for all values of  $K_2$ . These minimal curves occur near  $K_3=1, K_4=0, K_5=1$  and  $K_6=0.25$  for all C-BC's (set 2 of Table 6) except BPBS; there are no zero crossings for the L-BC curves. If a surround field input voltage ( $K_4$ ) is added, the minimizing of the slopes occurs at  $K_3=1, K_4=0, K_5=1$  and  $K_6=0.25$  for BPRD, BPRS, BPGD, BPGS and BPBD (set 8 of Table 6), but at  $K_6=0.25$  for BPBS and BPYD (set 9 of Table 6), while BPYS (set 10 of Table 6) is minimized at  $K_6=1$ . Above this minimized curve,  $F_{ss}$  decreases with increasing values of  $K_2$ , while below this minimized curve  $F_{ss}$  increases with increasing values of  $K_2$ . As before, single-opponent C-BC's show reinforcement of center and surround fields, while double-opponent C-BC's show

Table 6. Minimizing of  $F_{ss}$  for  $BC(t)$ 's with varying values of  $K$ 's.

Set	BPRD	BPRS	BPGD	BPGS	BPBD	BPBS	BPYD	BPYS	LBC
1 A	+191.2	+191.2	+126.9	+126.8	+74.2	+74.2	+318.0	+318.0	+392.2
B	+60.9	+60.9	-3.4	-3.4	-56.1	-56.1	+57.4	+57.4	+1.3
2 A	-95.6	+0.9	-63.4	-159.9	-37.1	-402.9	-159.0	+206.8	-196.1
B	-30.4	+66.0	+1.7	-94.7	+28.1	-142.3	-28.7	+141.6	-0.6
3 A	-382.4	-189.4	-253.7	-446.7	-148.4	-880.0	-636.1	+95.5	-784.4
B	-121.7	+71.2	+6.9	-186.1	+112.3	-228.4	-114.9	+225.8	-2.6
4 A	-955.9	-570.0	-634.3	-1020	-370.9	-1834	-1590	-127.0	-1961
B	-304.4	+81.5	+17.2	-368.7	+280.6	-400.7	-287.1	+394.2	-6.5
5 A	-1051	-665.6	-697.7	-1083	-408.0	-1871	-1749	-286.0	-2157
B	-334.8	+51.1	+18.9	-367.0	+308.7	-372.6	-315.9	+365.5	-7.2
6 A	-1147	-761.2	-761.2	-1147	-445.1	-1908	-1908	-445.1	-2353
B	-365.2	+20.7	+20.7	-365.2	+336.8	-344.6	-344.6	+336.8	-7.8
7 A	+191.2	+191.2	+126.9	+126.9	+74.2	+74.2	+318.0	+318.0	+392.2
B	+60.9	+60.9	-3.4	-3.4	-56.1	-56.1	+57.4	+57.4	+1.3
8 A	+51.5	+148.0	+83.6	-12.8	+110.0	-255.8	-11.9	+353.9	-196.1
B	-29.9	+66.5	+2.2	-94.3	+28.5	-141.8	-28.3	+142.1	-0.1
9 A	-88.2	+104.8	+40.4	-152.5	+145.8	-585.8	-341.9	+389.7	-784.4
B	-120.8	+72.2	+7.9	-185.1	+113.2	-227.4	-113.9	+226.8	-2.6
10 A	-367.6	+18.3	-46.0	-431.9	+217.4	-1246.0	-1002.0	+461.3	-1961.0
B	-302.4	+83.5	+19.2	-366.7	+282.4	-398.8	-285.2	+396.1	-6.5
11 A	-463.2	-77.3	-109.4	-495.3	+180.3	-1282.0	-1161.0	+302.3	-2157.0
B	-332.8	+53.0	+20.9	-365.0	+310.7	-370.7	-313.9	+367.4	-7.2
12 A	-558.7	-172.8	-172.8	-558.7	+143.3	-1320.0	-1320.0	+143.3	-2353.0
B	-363.3	+22.6	+22.6	-363.3	+338.7	-342.6	-342.6	+338.7	-7.8

Note: For Sets, A and B signify  $K_2=0$  and 100, respectively.

Sets 1-4,  $K_3=1, K_4=0, K_5=1$  while  $K_6$  or  $K_8$  varies with 1=0, 2=0.25, 3=0.5, 5=1.

Sets 5-6,  $K_3=1, K_4=0, K_6$  or  $K_8=1$  while  $K_5$  varies with 5=0.5, 6=0.

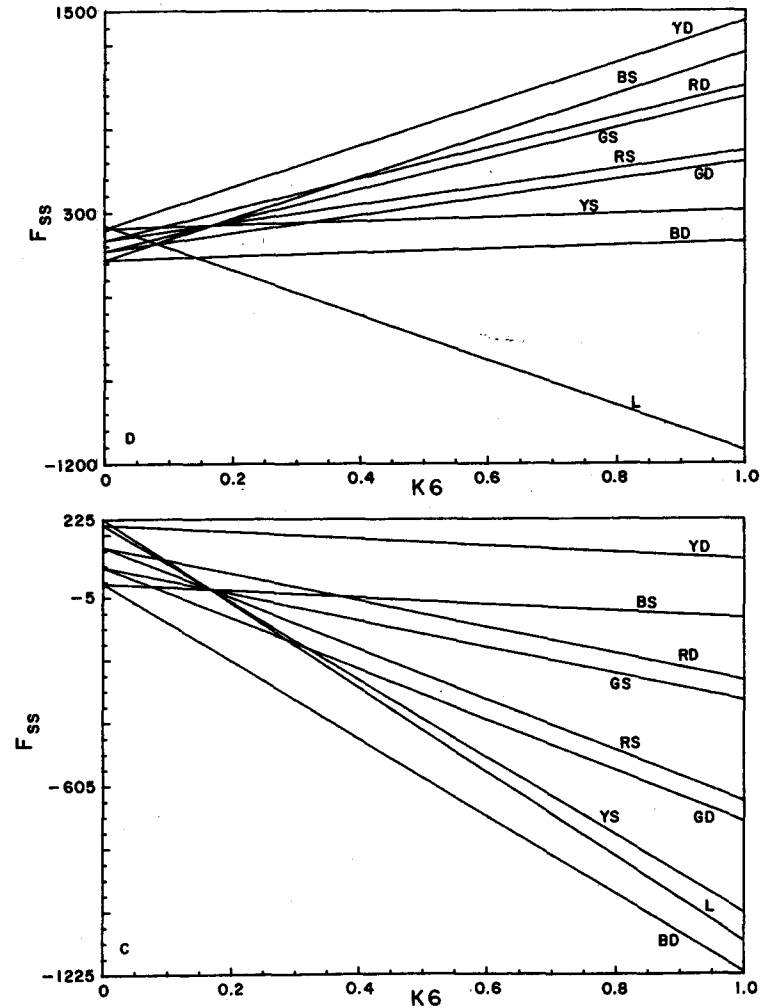
Sets 7-10,  $K_3=1, K_4=0.25, K_5=1$  while  $K_6$  or  $K_8$  varies with 7=0, 8=0.25, 9=0.5, 10=1.

Sets 11-12,  $K_3=1, K_4=0.25, K_6$  or  $K_8=1$  while  $K_5$  varies with 11=0.5, 12=0.

cancellation (Table 6) for C-BR and C-BY, but the opposite effects for C-BG and C-BB.

Effects of varying surround field input voltage on  $F_{ss}$ 's

With  $K_4=0$ , all slopes are negative, i.e.  $F_{ss}$  decreases as  $K_6$  is increased (Fig. 13C). For single-opponent C-BC's and L-BC, all curves go through an isoelectric point at  $K_6=0.16$  with  $K_2=0, K_3=1, K_4=0$  and  $K_5=1$  (Fig. 13C). With  $K_4=1$ , i.e. with an antagonistic L-HC input voltage now present, all slopes except those for L-BC are positive (Fig. 13D), but the isoelectric point is unchanged. Double-opponent C-BC's



form sets of diverging curves whose isoelectric point is to the left of  $K_6=0$ ; now, however, the curves for L-BC do not go through the same isoelectric point as does the curves for the single-opponent C-BC's (Fig. 13D).

#### Roots

When  $K_2K_3$  is below the 1st critical level,  $PX(t)$  is described by a linear cascade of 4 exponential curves:

$$PX(t) = A + B\exp(-at) + C\exp(-bt) + D\exp(-rt) + E\exp(-ut),$$

where  $-a$ ,  $-b$ ,  $-r$  and  $-u$  are the roots of the quartic equation (Part A),

$$s^4 + as^3 + bs^2 + cs + d = 0.$$

At the 1st critical value,  $-r$  and  $-u$  merge to form  $-v$  and the equation becomes that of a critically damped curve:

$$(B + Ct)\exp(-vt).$$

At the 2nd critical value,  $-a$  and  $-b$  merge to form  $-c$  and its equation is that of a critically damped wave:

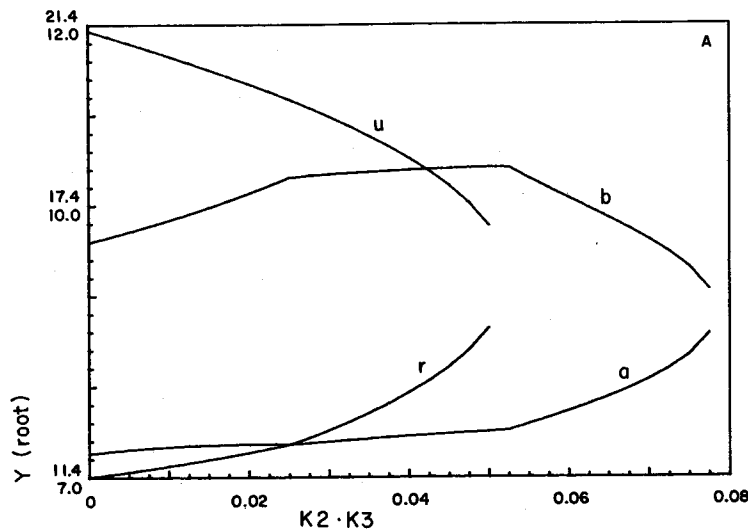


Fig. 14. Effects of varying gain factors on roots of quartic equation. Except for indicated changes,  $T_r$ ,  $T_g$ ,  $T_b$  and  $T_c$  are 0.09, 0.1, 0.14 and 0.047 sec, respectively. *A* displays effects of increasing negative feedback on the 2 sets of roots of quartic equation. *x*-axis represents increasing values of  $K_2$ , while *y*-axis represents 2 sets of values of roots; upper set refers to  $-u$  and  $-r$  and lower set refers to  $-a$  and  $-b$ . *B* and *C* display effects of varying  $T_c$  (*x*-axis) on roots  $-u$  and  $-r$  (*B*) and  $-a$  and  $-b$  (*C*). Each root is represented by set of 5 curves dependent on  $K_2K_3$ . Innermost curve represents plot with  $K_2K_3=0.05$  with an orderly procession inwards of  $K_2K_3=0.04$ , 0.03, 0.02 and 0.01, respectively. *D* displays effects of altering  $T_r$  on roots  $-a$  and  $-b$  for indicated values of  $K_2K_3$ , i.e. 0.01, 0.02 and 0.05.

$$(D + Et)\exp(-ct).$$

Above the 2nd critical value,  $PX(t)$  is described by the linear addition of 2 damped sine waves (Part A):

$$PX(t) = A + B\exp(-ct)\sin(ft + \phi_1) + C\exp(-vt)\sin(wt + \phi_2).$$

Roots are functions of the 4 time constants,  $T_r$ ,  $T_g$ ,  $T_b$  and  $T_c$ , as well as the 2 gain factors  $K_2$  and  $K_3$  which control the negative feedback path. The relationship between  $K_2K_3$  and the roots is complicated (Fig. 14A). For the 1st pair of roots ( $-r$  and  $-u$ ), as  $K_2K_3$  increases, the values of the roots converge and end at the critical value of  $K_2K_3 > 0.05$  with the value of  $-v = 15.86$ . The values of the 2nd pair of roots ( $-a$  and  $-b$ ) increase somewhat until the 1st critical level and then decrease to  $-c = 8.80$  at the 2nd critical level of  $K_2K_3 > 0.0775$  (Fig. 14A). L-HC (with  $T_c$ ) has the lowest time constant (Table 1). The 1st set of roots start at widely divergent values (Fig. 14B) with  $T_c = 0.02$  sec and with the other  $T_x$ 's kept constant at higher values than 0.02. As  $T_c$  increases the values of the roots converge with  $-u$  changing more than  $-r$ . When  $K_2K_3 = 0.01$ , the values of  $-r$  and  $-u$  fuse to  $-v$  at  $T_c > 0.06$  sec. Increasing  $K_2K_3$  decreases  $-u$  and increases  $-r$ , thereby, resulting in a smaller value of  $T_c$  at which the critically damped value of  $-v$  is obtained (Fig. 14B). The 2nd pair of roots ( $-a$  and  $-b$ ), which have the higher critical value, behave somewhat differently (Fig. 14C). As  $T_c$  is increased, the values of the roots initially increase and only when  $T_c$  is greater than the value of the 1st set of roots (i.e.  $-r$  and  $-u$ ) does the 2nd pair of roots converge to  $-c$ . At first, increasing  $K_2K_3$  produces increases in the values of the roots  $-a$  and  $-b$ , but as with the 1st set of roots, the critical value is reached at lower values of  $T_c$ . Fig. 14D demonstrates the effects of varying  $T_r$  on the 2nd set of roots (i.e.  $-a$  and  $-b$ ). With  $T_r = 0.05$  sec, which is the approximate value of  $T_c$ , the 2 roots are

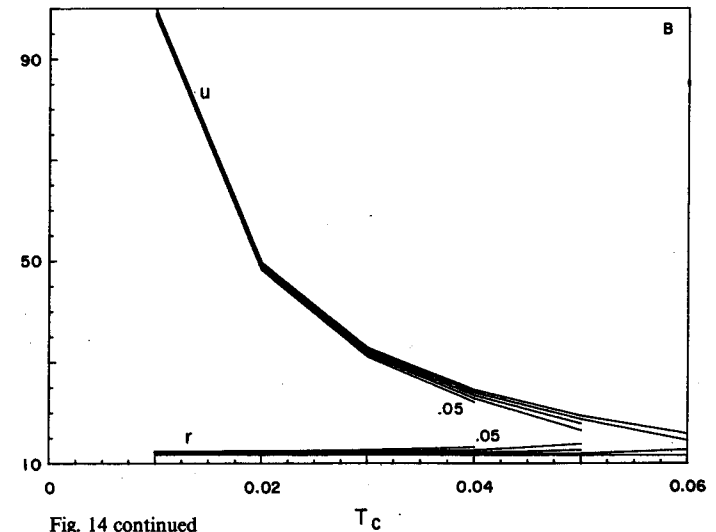


Fig. 14 continued

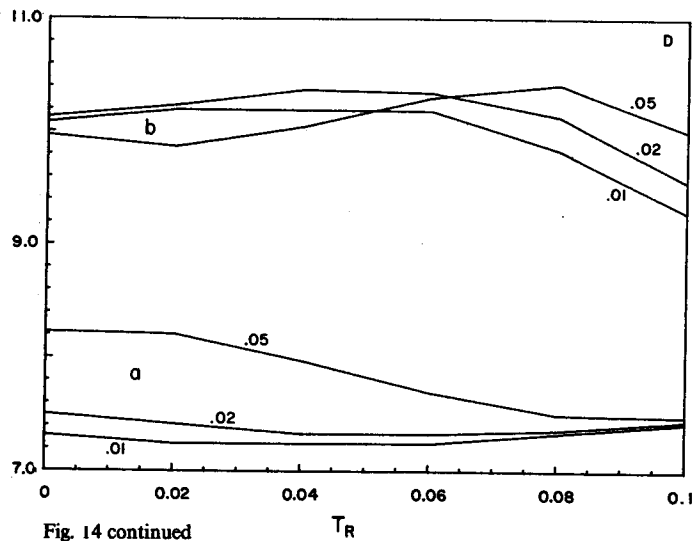
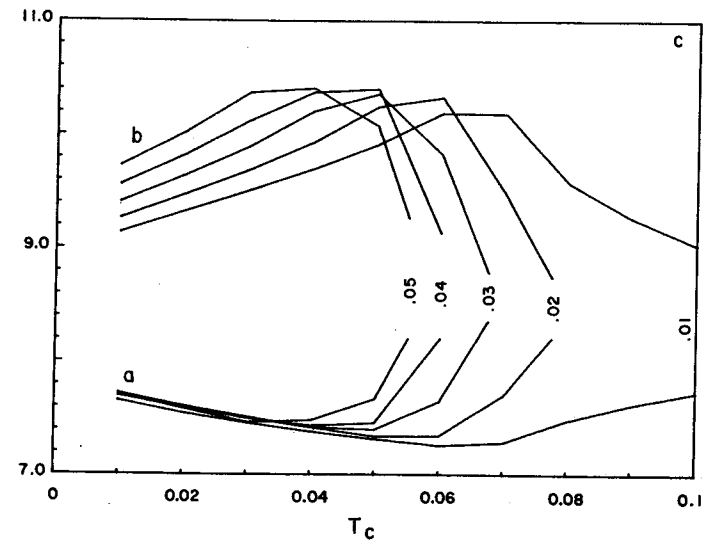


Fig. 14 continued

closest together with  $K_2K_3 = 0.05$  and furthest apart with  $K_2K_3 = 0.01$ . Increasing  $T_r$  does not radically change the values of the roots, but at  $T_r = 0.1$  sec, which is the value of  $T_g$ , the 2 roots are closest together with  $K_2K_3 = 0.01$  and the furthest apart with  $K_2K_3 = 0.05$ . Changing any other time constant for the PC's produces similar effects. The one generalization to be made is that changing the time constant of the lowest-valued element has the largest effect and the further apart this lower value is

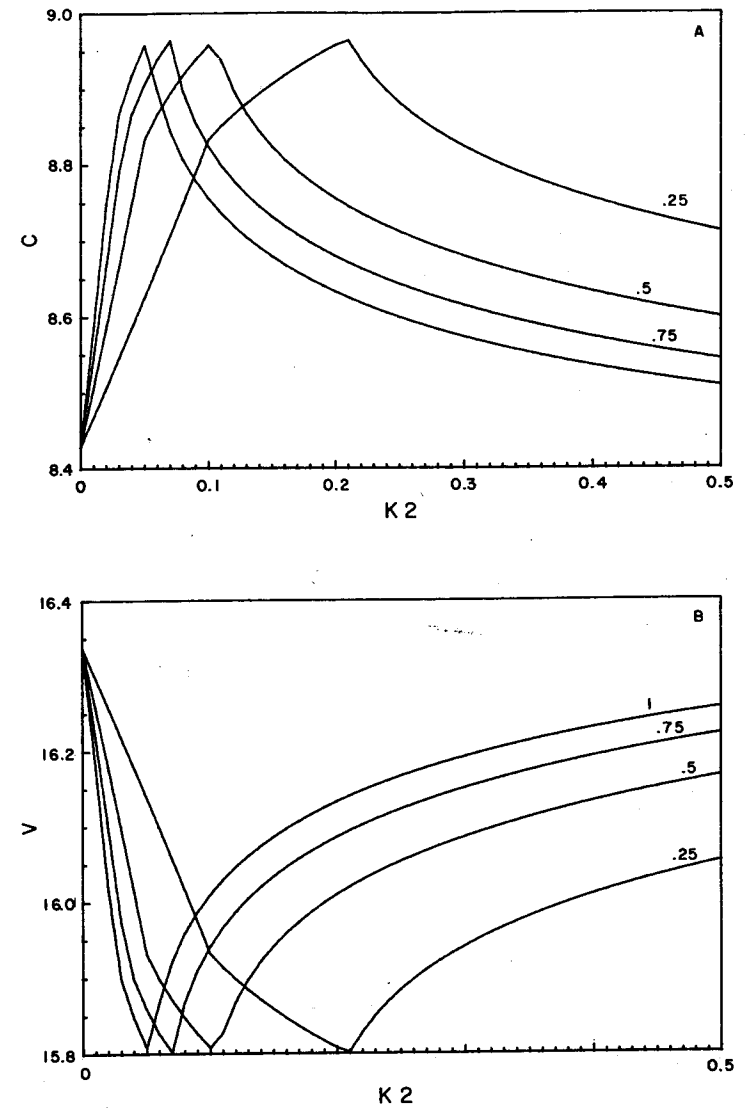


Fig. 15. Effects of increasing negative feedback on values of roots at critical levels. A and B display effects of negative feedback (x-axis) on value (y-axis) of critically damped roots  $-c$  (A) and  $-v$  (B). Numbers designating curves represent values of  $K_3$ .  $T_R$ ,  $T_G$ ,  $T_B$  and  $T_C$  are 0.09, 0.01, 0.14 and 0.04 sec, respectively. C and D display effects of negative feedback on values of critically damped roots  $-v$  (C) and  $-c$  (D) with 5 indicated values of  $T_C$  and  $T_R$ ,  $T_G$  and  $T_B$  are 0.08, 0.1 and 0.14 sec respectively.

from the time constants of the other elements, the greater will be the effects of the change in value of the lowest element.

The values of the critically damped roots  $-c$  and  $-v$  do not remain constant as  $K_2K_3$  is increased (Fig. 15A, B). The values of  $-c$  and  $-v$  are initially imaginary and do not become real until the critical levels are reached at which points the values of

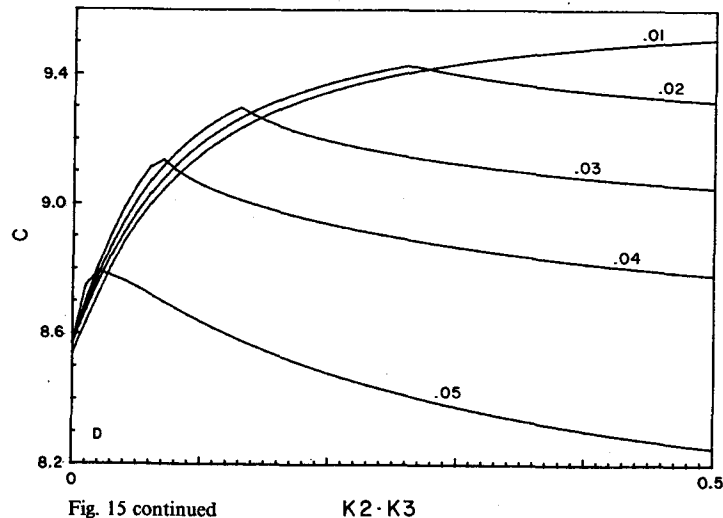
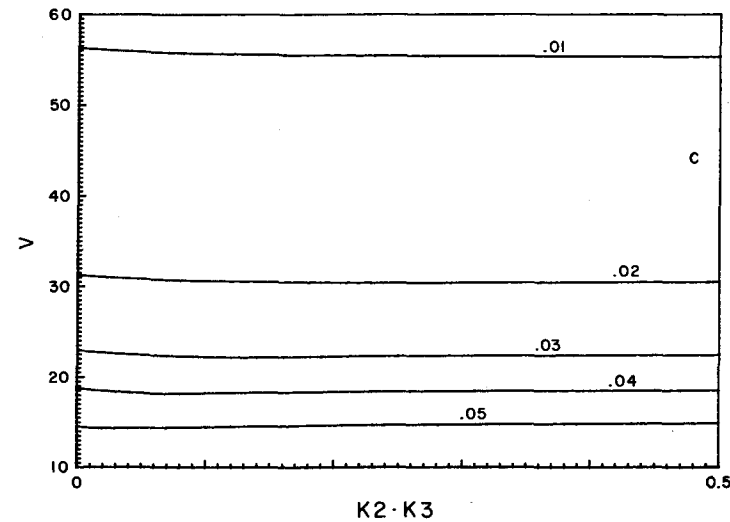


Fig. 15 continued

K2 · K3

$-c$  decreases and  $-v$  increases as  $K_2K_3$  increases.

Finally, increasing  $T_c$  to approach the value of  $T_r$  radically alters the absolute values of  $-v$  (Fig. 15C), but alters  $-c$  only moderately (Fig. 15D). The critical level of  $K_2K_3$  increases as  $T_c$  decreases. Again as with  $-a$ ,  $-b$ ,  $-r$  and  $-u$ , the greatest changes in  $-c$  and  $-v$  occur when the lowest valued time constant is changed and the further this  $T_x$  is from the others, the greater is the change.

## 4. Discussion

### 4.1 Introduction

It should be emphasized that the model has a basis in both physiological and anatomical data as pointed out in my 1st theoretical paper where the details of the synthesis of the literature was discussed (Siminoff, 1980a). Thus, 3 cone-types, opponent color pairs, L- and C-types of HC's and BC's and single- and double-opponent elements have been described in the literature. Anatomical and circuitry data are in fair agreement with the model, but with some variations as is pointed out in a later section dealing with triphasic C-HC's. The major assumption that I make is that the spatial organization of the cone retina is precise and inputs to higher elements can be defined geometrically by the unit hexagon. It cannot be overly emphasized that no given species of vertebrate has all of the features of the generalized model, but rather the model acts as a spine from which the retina of any given animal can be simulated by proper choice of elements and parameters. The model is essentially simple and complexities of  $F(t)$ 's come about naturally due to the interplay of antagonistic inputs with differing time courses, negative feedback, etc.

### 4.2 Steady states

Formulas for steady state values are found by dropping out time-dependent terms in  $F(t)$ 's and are presented in Table 10 of Part A. These formulas are similar to the polarization factors derived in my 1st theoretical paper, but with modifications resulting from the differences in approaches to derivations of the equations. In the present form,  $F(t)$  for the direct cone input is modified by the factor:

$$(1 + 2K_2K_3)/(1 + 3K_2K_3),$$

while  $F(t)$ 's for the indirect cone inputs are modified by:

$$(K_2K_3^2)/(1 + 3K_2K_3).$$

Steady state values depend on the resultant of antagonistic inputs, each weighted by its synaptic gain.

Also involved in determining  $F_{ss}$ 's is the input parameter,  $W_x$ , i.e. the number of cones ( $N_x$ ) multiplied by the intensity ( $Y_x$ ). Intensity factors are dependent on the numbers of each cone-type in the UH and the total energy of light falling on the cones weighted by the univariance of the cones and stray light. Variations of cone-types and sloppy filter properties of cones have been previously discussed (Siminoff, 1980a, b, 1981). The relative dominance of cones plays an important role in determining  $F_{ss}$ ,

both as to the direct cone inputs and indirect cone inputs via negative feedback.

Stray light effects, electrical coupling of cones and electrical coupling of HC's are not taken into account in the present study. Previous studies involving electronic models (Siminoff, 1984b) showed that these factors do not affect the model's dynamics, but rather the *dc* level ( $F_{ss}$ ). These factors become part of the weighted input,  $A_x$ , which modifies  $W_x$ , i.e.  $A_x W_x$ .

Figs. 10–13 demonstrate the effects of the various parameters on  $F_{ss}$ . Cones, which are normally hyperpolarized by light, can be adjusted to become depolarized by light (Fig. 10). Relative dominance of cone-types is an important factor and via feedback the most dominant cone-type can swamp the effects of the other cone-types.

Color-coding of C-HC's can also be made to vary by the adjustment of a number of parameters such that the normally biphasic coding of the antagonistic color pairs can be radically altered; this has been borne out in studies with an electronic model (Siminoff, 1984b). Analysis of the turtle cone retina (Siminoff, 1980b) demonstrates this alteration of color-coding, and this was confirmed by a comparison with the literature. The number of parameters that can alter  $F_{ss}$  increases at the BC level; the gains of the 2 antagonistic inputs ( $K_5$  and  $K_6$  or  $K_8$ ) are probably the most important of these factors (Fig. 13). Color-coding of C-BC's can be radically altered by variations of these factors as well as the other factors already discussed. The L-channel is not color-coded and thereby, is less affected by variations of the parameters, although absolute levels are changed.

Cones are linear at weak flashes, but non-linear in response to strong flashes (Baylor and Fuortes, 1970; Baylor *et al.*, 1971, 1974; Baylor and Hodgkin, 1973, 1974; Burkhardt, 1977; Fain and Dowling, 1973; Fuortes *et al.*, 1973; Lasansky and Marchiafava, 1974; Pasino and Marchiafava, 1976), and are sloppy filters with overlapping absorption spectra (Baylor and Hodgkin, 1973; Naka and Rushton, 1967; Tomita, 1978). However, for electronic models (Siminoff, 1983a, 1984b), simulated cones show power functions for intensity-response curves and this non-linearity is avoided in system analysis by considering cone outputs as the input factors,  $Y_x$ 's, which were determined by the electronic simulation. Thus any intensity-response relationship can be assumed by use of values of  $Y_x$  dependent on specific relationships to intensity.

### 4.3 Dynamic state

One generalization that can be made about my model is that the dynamic characteristics of the system are governed by the interplay of antagonistic time-dependent voltages of differing time courses serving as inputs to elements acting as simple low-pass filters. Transients of varying degrees appear at the ON and OFF phases of the responses to step input voltages. An offshoot of this is that the equation, which describes the dynamics of the system, originates at the cones due to negative feedback loops (Part A). This equation is carried through up to and including the BC's (Table 1 of Part A).

I have assumed that there are no feedback pathways from AC's to either BC's or HC's. Effects of feedback loops from AC's to BC's and HC's have been studied using a

$43 \times 41$  electronic model (Siminoff, 1984c) and the results indicate that such feedback pathways do not alter the current conclusions, but rather, these higher order feedback loops add onto the system in a predictable fashion.

### Time Constants

The generalized vertebrate cone retina is best described by either cascading exponential curves or cascading damped sine waves that are dependent on the amounts of negative feedback from L-HC to cones. Time constants for cones and L-HC are involved in these feedback loops and the form of the Laplace transforms depend on the number of differing time constants. Regardless, equations for  $F(t)$ 's describe cascading exponentials. Above the critical level and dependent on  $K_2 K_3$  (Part A),  $F(t)$ 's describe cascading damped sine waves, but otherwise follow similar principles as when  $K_2 K_3$  is below the critical level.

The further apart the time constants of the elements involved, the more pronounced are the effects of negative feedback on the dynamic properties of the model (Figs. 14, 15). As these values approach each other, the values of the roots also approach each other and eventually lead to a single exponential curve or single damped sine wave. One consequence of having 4 separate time constants is that oscillations will occur at lower values of  $K_2 K_3$ . Time constants of BC's, etc. have no such effects and only add to  $F(t)$  additional exponential terms weighted by gain factors.

### Cones

$F(t)$ 's for cones are highly dependent on such factors as relative cone dominance, time constants and spectral distribution of light stimuli (Figs. 1, 2). As a general principle, negative feedback decreases hyperpolarization of the cones and the exact shape of  $F(t)$  will depend on the time relationships between the direct cone input, the indirect cone inputs via negative feedback and the invariance of the cones. Thus, negative feedback can produce flattening of the initial phases (Fig. 1A) or overshoots (Fig. 2C). If the time constant of L-HC, which is the source of negative feedback, is longer than the time constant of the direct cone input, then the waveforms of  $PC(t)$  has typically overshoots. True oscillations due to damped sine waves (Fig. 1) appear on  $PX(t)$ 's only a fairly high values of  $K_2 K_3$  (i.e. 0.5 or greater). Table 7 lists the generalized equations for the transient responses of various retinal elements derived by dropping out the steady state portion (i.e. A's) of  $F(t)$ 's in Tables 4, 8 and 9 of Part A. For  $K_2 K_3 = 0$ ,  $PX(t)$ 's show pure exponential waveforms, but when  $K_2 K_3 = 0.25$ ,  $PX(t)$ 's have either cascading exponential or cascading sine wave as the waveform with the coefficients determined by the direct cone input ( $X$ ) reduced by weighted factors of the indirect cone inputs (i.e.  $Y, Z$ ). If  $Y$  or  $Z$  dominates, as is the case with red-dominant retinas, then  $PX(t)$  can be dominated by the indirect input to produce depolarization.

I have reviewed the literature related to the roles of near-field enhancement and far-field inhibition of  $F_{ss}$ 's of PC's, particularly as applied to the turtle retina (Siminoff, 1980b), so that only the dynamic aspects of  $PX(t)$ 's will be discussed.

Table 7. Transient state equations.

Element	$K_2, K_3$	Equation
PX(t)	0 <CL >CL	$k_1 \exp(-X \cdot t)$ $I_1 [BX(1 - a_1) \exp(-a \cdot t) + CX(1 - a_2) \exp(-b \cdot t) + DX(1 - a_3) \exp(-r \cdot t) + EX(1 - a_4) \exp(-u \cdot t)]$ $m_1 [QX(1 - a_1) \exp(-c \cdot t) \sin(f \cdot t + \theta_1) + RX(1 + a_2) \exp(-v \cdot t) \sin(w \cdot t + \theta_2)]$
LH(t)	0 <CL >CL	$k_2 [BR \exp(-J \cdot t) + BG \exp(-K \cdot t) + BB \exp(-L \cdot t) + C \exp(-G \cdot t)]$ $I_2 [B(1 - \beta) \exp(-a \cdot t) + C(1 - \beta_2) \exp(-b \cdot t) + D(1 - \beta_3) \exp(-r \cdot t) + E(1 - \beta_4) \exp(-u \cdot t) + F(1 - \beta_5) \exp(-G \cdot t)]$ $m_2 [Q(1 - \beta) \exp(-c \cdot t) \sin(f \cdot t + \theta_1) + R(1 - \beta_2) \exp(v \cdot t) \sin(w \cdot t + \theta_2) + S(1 - \beta_3) \exp(-G \cdot t)]$ $C = CR + CG + CB, \text{ etc}$
CHX(t)	0 <CL >CL	$k_3 [BX(1 - a_1) \exp(-X \cdot t) - a_2 \cdot BY \exp(-Y \cdot t) - a_3 \cdot BZ \exp(-Z \cdot t) + C(1 - \beta) \exp(-G \cdot t)]$ $I_3 [B(1 - \gamma) \exp(-a \cdot t) + CX(1 - \gamma_2) \exp(-b \cdot t) + DX(1 - \gamma_3) \exp(-r \cdot t) + EX(1 - \gamma_4) \exp(-u \cdot t) + FX(1 - \gamma_5) \exp(-G \cdot t)]$ $m_3 [QX - \gamma_1 \cdot Q] \exp(-c \cdot t) \sin(f \cdot t + \theta_1) + (RX - \gamma_2 \cdot R) \exp(-v \cdot t) \sin(w \cdot t + \theta_2) + (SX - \gamma_3 \cdot S) \exp(-G \cdot t)]$ $\beta = f(X, Y, Z, t)$
LBC(t)	0 <CL >CL	$k_4 [BR(1 - \gamma) \exp(-J \cdot t) + BG(1 - \gamma_2) \exp(-K \cdot t) + BB(1 - \gamma_3) \exp(-L \cdot t) + (C - a_3) + [D - \gamma_4] \exp(-G \cdot t)]$ $I_4 [B(1 - \delta) \exp(-a \cdot t) + C(1 - \delta_2) \exp(-b \cdot t) + D(1 - \delta_3) \exp(-r \cdot t) + E(1 - \delta_4) \exp(-u \cdot t) + F(1 - \delta_5) \exp(-G \cdot t)]$ $m_4 [Q(1 - \delta) \exp(-c \cdot t) \sin(f \cdot t + \theta_1) + R(1 - \delta_2) \exp(-v \cdot t) \sin(w \cdot t + \theta_2) + S(1 - \delta_3) \exp(-G \cdot t)]$
BPXD(t)	0 <CL >CL	$k_5 [BX(1 - \delta_1 + \epsilon_1) \exp(-X \cdot t) + \epsilon_2 \cdot BY \exp(-Y \cdot t) + \epsilon_3 \cdot BZ \exp(-Z \cdot t) + CX(1 - \lambda) \exp(-G \cdot t)]$ $I_5 [(BX - \delta_1 \cdot B) \exp(-a \cdot t) + (CX - \delta_2 \cdot C) \exp(-b \cdot t) + (DX - \delta_3 \cdot D) \exp(-r \cdot t) + (EX - \delta_4 \cdot E) \exp(-u \cdot t) + (FX - \delta_5 \cdot F) \exp(-G \cdot t)]$ $m_5 [QX - \delta_1 \cdot Q] \exp(-c \cdot t) \sin(f \cdot t + \theta_1) + (RX - \delta_2 \cdot R) \exp(-v \cdot t) \sin(w \cdot t + \theta_2) + (SX - \delta_3 \cdot S) \exp(-G \cdot t)]$ $\lambda = f(X, Y, Z, t)$
BPXS(t)	0 <CL >CL	$k_6 [BX(1 - \epsilon_1) \exp(-X \cdot t) - (\delta_2 + \epsilon_2) BY \exp(-Y \cdot t) + \epsilon_3 \cdot BZ \exp(-Z \cdot t) + CX(1 - \lambda) \exp(-G \cdot t)]$ $I_6 [(BX - \lambda_1 \cdot B) \exp(-a \cdot t) + (CX - \lambda_2 \cdot C) \exp(-b \cdot t) + (DX - \lambda_3 \cdot D) \exp(-r \cdot t) + (EX - \lambda_4 \cdot E) \exp(-u \cdot t) + (FX - \lambda_5 \cdot F) \exp(-G \cdot t)]$ $m_6 [QX - \lambda_1 \cdot Q] \exp(-c \cdot t) \sin(f \cdot t + \theta_1) + (RX - \lambda_2 \cdot R) \exp(-v \cdot t) \sin(w \cdot t + \theta_2) + (SX - \lambda_3 \cdot S) \exp(-G \cdot t)]$

Vertebrate cone responses to light flashes (ca. 10 msec in duration) are typically transient hyperpolarizations, with the peak time getting shorter with increasing intensity, and invariably the decay time is longer than the rise time (Baylor and Fuortes, 1970; Baylor *et al.*, 1971; Baylor and Hodgkin, 1973, 1974; Lasansky and Marchiafava, 1974; Pasino and Marchiafava, 1976). With increasing intensity, a slower repolarization phase appears with prolonged decay time of up to 0.5 sec. Negative feedback from L-HC is present in most species that have been studied and causes the decay time to decrease. At low intensities, nevertheless, cones act as low-pass filters (Tranchina *et al.*, 1981), which is consistent with my simulated PC's. However, there are discrepancies. My simulated PC's are pure low-pass filters, so that the OFF phase is the mirror image of the ON phase, while actual cones show longer decay phases even at low intensities. There appear to be a number of time-dependent factors that alter the characteristics of cone responses to differing intensities and differing times after the stimulus (Baylor and Hodgkin, 1974; Baylor *et al.*, 1974; Normann and Perlman, 1979a). If long duration stimuli are used that permit establishment of equilibrium (Baylor and Hodgkin, 1973, 1974; Cervetto, 1973; Fuortes *et al.*, 1973; Normann and Perlman, 1979a; O'Bryan, 1973), cone responses show initial transients and have plateaus similar to those of Figs. 1 and 2, but the OFF phases are still somewhat prolonged. Time-dependent changes in sensitivity and adaptation appear in real cones (Baylor and Hodgkin, 1973, 1974; Normann and Perlman, 1979a; Normann and Werblin, 1974; Pinto and Pak, 1974a, b), which have not been included in my model, but do not seriously affect the results presented here with its limitations on conditions. Thus, my simulated cones are only approximations of real cones, more so at the lower intensities and for stimulus durations greater than the time constant of the cones, i.e. >150 msec.

Horizontal Cells

L- and C-HC's are organized differently and therefore differ in response patterns (Figs. 3-6, Table 2), so that it is convenient to discuss them separately.

L-HC's

From Table 7, it can be seen that the transient states of L-HC's are similar to those of PC's, differing in that all 3 cone-types contribute direct input voltages, and there is an additional contribution from the time constant of L-HC. Thus, LH(t) is flat for the first 20 msec or so depending on the value of  $T_c$  (i.e. the time constant of L-HC).

As predicted, L-HC is dynamically similar to the cones taking into account the slower time course of L-HC (Cervetto and MacNicholl, 1972; Cervetto and Piccolino, 1974; Fuortes and Simon, 1974; Lasansky and Vallergera, 1975; Nelson, 1977; Normann and Perlman, 1979b; Pasino and Marchiafava, 1973; Piccolino *et al.*, 1981; Saito *et al.*, 1974; Simon, 1973, 1974; Toyoda *et al.*, 1978; Werblin and Dowling, 1969). Responses to brief pulses are similar to cones showing a faster rise time than decay time; decay time increases with intensity. L-HC show transient ON responses, dependent on intensities with labile OFF responses. Although all wavelengths evoke hyperpolarization of L-HC, time courses vary depending on

wavelength, which is consistent with the results of simulation (Fig. 5A). All data are consistent with the proposition that L-HC act as a linear low-pass filter reflecting the PC( $t$ ), but with a slower time course. While these general patterns agree with my model, details vary from animal to animal as to be expected from the number of variables that are involved (Table 1). In mammalian retinas, rods and cones converge onto the same L-HC (Nelson, 1977); Foerster *et al.*, 1977), while in lower vertebrates, such as teleost fishes, there are separate cone and rod L-HC's (Kaneko and Yamada, 1972; Teranishi *et al.*, 1982; Toyoda and Tonosaki, 1978; Wu and Dowling, 1980). There appear to be several types of L-HC's in a given animal with differing receptive field sizes that may differ in feedback circuitry (Fuortes and Simon, 1974; Lasansky and Vallerger, 1975; Neyton *et al.*, 1981; Normann and Perlman, 1979b; Piccolino *et al.*, 1981; Saito *et al.*, 1974; Simon, 1973; Yazulla, 1976).

L-HC responses to small stimuli, which are much smaller than cone responses at equivalent intensities, grow linearly with increasing radius of light spot (Naka, 1972); these findings lead one to conclude that the gain factor  $K_3$  is relatively small and spatial summation via electrical coupling of like-HC's contributes the major portion of the amplitude of L-HC's response. Thus  $K_2K_3$  is probably small in real retinas, which may explain why true oscillations are not prominent.

### C-HC's

C-HC's are more complex than L-HC's due to the presence of an antagonistic input voltage from L-HC with a slower time course than the direct cone input (Table 7). The antagonistic surround field introduces a biphasic opposing input voltage of a slower time course, so that the interplay of the 2 input voltages leads to complex transients dependent on the time relationships of the contributing elements (Table 7).

Negative feedback plays a dual role in evoking transients. On the one hand, as  $K_2K_3$  increases, the amplitude of the damped sine wave increases (Fig. 6), while on the other hand, coefficients  $A$ ,  $B$ , etc. for the transient equations of state (Table 7) are decreased by increasing values of  $K_2K_3$ . These opposing effects tend to reduce oscillations as has been observed.

While L-HC's have been studied extensively, C-HC's have been less studied particularly as related to their dynamic characteristics. Response dynamics of biphasic C-HC's are consistent with my model (Fuortes and Simon, 1974; Kato, 1979; Saito *et al.*, 1974; Shigematsu *et al.*, 1978; Yang *et al.*, 1982; Yazulla, 1976; Wu and Dowling, 1980). Latency measurements of color-coded S-potentials in carp retina were made by cross-correlation techniques (Shigematsu *et al.*, 1978). The biphasic C-HC,  $G-R+$  responds to green, blue and yellow monochromatic lights with hyperpolarization that has a shorter time course than the depolarizing wave due to red monochromatic lights. For C-HC,  $B-Y+$ , similar results are seen, with blue light giving hyperpolarizing responses that have the shortest time courses, while red and yellow colored lights give slower depolarizing responses. Green light gives biphasic responses with hyperpolarization appearing initially followed by depolarization. A triphasic C-HC was described that was similar to the biphasic C-HC,  $B-Y+$ , except for a hyperpolarizing red response that looked slower in time course than the

depolarizing yellow response. These results along with those of Spekrijse and Norton (1970) are taken as evidence for the cascading model of Lipetz (1978) for triphasic C-HC's. My simulated biphasic C-HC's can be triphasic due to negative feedback (Siminoff, 1980a, b). The experimental data is consistent with C-HC's acting as linear low-pass filters as proposed in my model.

### Bipolar Cells

The controlling factors for the dynamic states of BC's are increased over PC's and HC's; not only are there those parameters involved with the 2 antagonistic input voltages, but there are the additional factors which control the balance between these 2 input voltages as well as the additional delay for the BC( $t$ )'s. Thus, BC's display more variabilities as to the presence of transients (Figs. 7-9, Table 3, 4). In terms of transients resulting from increasing  $K_2K_3$ , direct center field input voltages add positive waves (Fig. 7A), while surround field input voltages add large negative waves with faster time courses. Mixed center and surround field inputs lead to complex balances of positive and negative waves of differing time courses arising from antagonistic input voltages. Besides gain factors, intensity factors play important roles in shaping BC( $t$ )'s (Fig. 8) and in general, the dominant cone-type, if one is present, is crucial for BC( $t$ )'s.

These complex interplays of antagonistic input voltages, which in turn are the resultant of interplay of antagonistic input voltages, are reflected in the equations of state (Table 7). For  $K_2K_3$  greater than the critical level, negative feedback to all 3 cone-types is synergistic and produce large overshoots to BC's.

Literature pertaining to the dynamic properties of BC's is limited and most studies deal with the effects of steps of white light in undefined HPBC's or DPBC's. One generalization that can be made is that the responses of BC's to steps of white light are quite variable and quite often HPBC responses are not complete mirror images of the DPBC responses; usually DPBC responses are more typical with ON and OFF transients, while HPBC responses tend to show less transients (Naka, 1972; Kaneko, 1973; Kato and Negishi, 1979; Mitarai *et al.*, 1978; Naka *et al.*, 1975; Naka and Ohtsuka, 1975; Richter and Simon, 1975; Schwartz, 1974; Wunk and Werblin, 1979). Center field responses tend to have less transients and the addition of surround field input voltages lead to transient ON and OFF phases as demonstrated in my model (Figs. 7, 8). There are data in the literature that  $F(t)$ 's of DPBC's and HPBC's have differing time course (Frumkes and Miller, 1979; Marchiafava and Torre, 1978). There is no significant literature pertaining to the dynamic properties of C-BC's; at least that which can be used to compare with my model.

### Other Models

A number of computational models, which usually are restricted to specific species of vertebrates, have been described and have one important feature in common, i.e. transients, as in my model, arise from time differences of inputs (Abermethy, 1974; Fukurotani and Hara, 1975a, b, 1976; Hara and Kurose, 1976; Hara and Takabayshi, 1976; Kaneko and Naka, 1980; Powers and Arnett, 1981; Richter and Illman, 1982)

These computational models use fairly sophisticated transfer functions based on experimental data. My own model uses only one simple transfer function, i.e. a low-pass filter, and  $F(t)$ 's are generated by the spatial and temporal characteristics of the organization of the retina. Thus, my model has the advantage of demonstrating how the transfer functions are generated and the roles played by the various factors going into the organization of receptive fields.

## 5. Conclusions

A functional model of the generalized vertebrate cone retina has been presented (Part A) along with a detailed analysis (Part B). Photoreceptors are simulated by phototransistors that act as low-pass filters. Response characteristics of these simulated cones deviate from the known properties of real cones, particularly for brief flashes of light. With longer steps of light, deviations are not so apparent and appear as slightly longer recovery phases than rise times. Other retinal elements act as linear low-pass filters that reflect the asymmetries of the cones. A hardware model of the cones that simulate real cone responses have been constructed (Vallerga *et al.*, 1980). However, there are major drawbacks to this model one of which is that light inputs must be simulated by computer driven current generators. Using a phototransistor with complicated circuitry to simulate real cones would be prohibitive in cost considering that a minimal cone mosaic for adequate simulation of ganglion cells contains about 1700 cones.

A survey of the literature on PC's, HC's and BC's reveals that the overall response patterns of these elements are readily simulated by my model. One is struck by the degree of variability in terms of the details of dynamic characteristics of  $F(t)$ 's particularly in terms of transients. Considering the large number of variables involved as well as other factors such as stray light, electrical coupling of PC's and electrical coupling of like-HC's, these variabilities are not surprising. Other factors such as statistical variations of parameters and environmental effects of the state of the retina have not been considered.

Electronic analogues with mathematical analysis can be useful tools. First, in terms of simulating retinas of individual animals, mathematical models can be used to quickly determine response characteristics to simple stimuli, while the electronic analogue (which takes time to construct) can be used to determine responses characteristics to spatially complicated stimuli. In the mathematical analysis, feedback from AC's to BC's or to BC's has been ignored, since such mathematical analyses are extremely complex. These questions of higher order feedback circuits can be best investigated with the electronic model.

The electronic model is a functional model of the retina and is capable of generating information concerning the visual world in terms of such parameters as presence or absence of an object in part of the visual field, size, shape, color, movement and direction, etc. With proper miniaturization of the electronic circuits, the model could be used in neural prosthesis as an aid to the blind. Since the electronic model processes visual information analogous to real retinas, the information generated could be utilized directly by the visual cortex. If 2 such cone mosaics are used, even binocular information could be generated.

It is obvious that experiments on any given animal can not generate the diversity of data presented in this study. The various parameters (Table 1) can not be readily manipulated physiologically, nor does any given animal have all of the elements of the generalized model. Nor are there adequate data for vertebrates so as to be able to perform simulation studies on specific animals. The turtle retina (Siminoff, 1980b) has been subjected to modelling (at least for  $F_{ss}$ 's), but even here the data for the various parameters are lacking and could be only approximated or assumed. In the present studies I started with several simple principles and was able to generate an almost infinite variety of response patterns for retinal elements. Thus, it stands to reason that by selection of the proper values for the parameters listed in Table 1, and the proper choice of elements to be included, the retina of any given species of vertebrate could be simulated.

## Acknowledgements

This work was carried out during a NRC-Naval Medical Research and Development Command Research Associateship.

## References

- Abernethy, J. D. (1974). A dynamic model of a two-synapse feedback loop in the vertebrate retina. *Kybernetik* **14**, 187-200.
- Baylor, D. A. and Fuortes, M. G. F. (1970). Electrical responses of single cones in the retina of the turtle. *J. Physiol. (Lond.)* **207**, 77-92.
- Baylor, D. A., Fuortes M. G. F. and O'Bryan, P. M. (1971). Receptive fields of cones in the retina of the turtle. *J. Physiol. (Lond.)* **214**, 265-294.
- Baylor, D. A. and Hodgkin, A. L. (1973). Detection and resolution of visual stimuli by turtle photoreceptors. *J. Physiol. (Lond.)* **234**, 162-198.
- Baylor, D. A. and Hodgkin, A. L. (1974). Changes in time scale and sensitivity in turtle photoreceptors. *J. Physiol. (Lond.)* **242**, 729-758.
- Baylor, D. A., Hodgkin, A. L. and Lamb, T. D. (1974). The electrical response of turtle cones to flashes and steps of light. *J. Physiol. (Lond.)* **242**, 685-727.
- Burkhardt, D. A. (1977). Responses and receptive-field organization of cones in perch retinas. *J. Neurophysiol.* **40**, 53-62.
- Cervetto, L. (1973). Influence of sodium, potassium and chloride ions on the intracellular response of turtle photoreceptors. *Nature* **241**, 401-403.
- Cervetto, L. and MacNichol, E. F. (1972). Inactivation of horizontal cells in turtle retina by glutamate and aspartate. *Science* **178**, 767-768.
- Cervetto, L. and Piccolino, M. (1974). Synaptic transmission between photo-receptors and horizontal cells in the turtle retina. *Science* **183**, 417-419.
- Fain, G. L. and Dowling, J. E. (1973). Intracellular recording from single rods and cones in the mudpuppy retina. *Science* **180**, 1178-1180.
- Foerster, M. H., Grind, W. A. van de and Grusser, O.-J. (1977). Frequency transfer properties of three distinct types of cat horizontal cells. *Exp. Brain Res.* **29**, 347-366.
- Frumkes, T. E. and Miller, R. F. (1979). Pathways and polarities of synaptic interactions in the inner retina of the mudpuppy: II. Insight revealed by an analysis of latency and threshold. *Brain Res.* **161**, 13-24.
- Fukurotani, K. and Hara, K.-I. (1975a). A dynamic model of the receptive field of L-cells in the carp retina. *Biol. Cybern.* **20**, 1-8.

- Fukurotani, K. and Hara, K.-I. (1975b). Dynamic characteristics of the receptive field of L-cells in the carp retina. *Vision Res.* **15**, 1403-1405.
- Fukurotani, K. and Hara, K.-I. (1976). A dynamic model of the receptive field of horizontal cells for monochromatic lights. *Biol. Cybern.* **21**, 221-226.
- Fuortes, M. G. F., Schwartz, E. A. and Simon, E. J. (1973). Colour-dependence of cone responses in the turtle retina. *J. Physiol. (Lond.)* **234**, 199-216.
- Fuortes, M. G. F. and Simon, E. J. (1974). Interactions leading to horizontal cell responses in the turtle retina. *J. Physiol. (Lond.)* **240**, 177-198.
- Hara, K.-I. and Kurose, M. (1976). A model for the mechanisms of sensitivity control in the submammalian vertebrate retina. *Biol. Cybern.* **22**, 121-128.
- Hara, K.-I. and Takabayashi, A. (1975). A dynamic model of retinal cells in the vertebrate retina. *Biol. Cybern.* **20**, 61-67.
- Kaneko, A. (1973). Receptive field organization of bipolar and amacrine cells in the goldfish retina. *J. Physiol. (Lond.)* **235**, 133-153.
- Kaneko, A. and Yamagata, M. (1972). S-potentials in the dark-adapted retina of the carp. *J. Physiol. (Lond.)* **227**, 261-273.
- Kato, S. (1979). C-type horizontal cell responses to annular stimuli. *Exp. Brain Res.* **28**, 627-639.
- Kato, S. and Negishi, K. (1979). Rod- and cone-bipolar cell responses in the carp retina. *Exp. Eye Res.* **28**, 159-166.
- Krausz, H. I. and Naka, K.-I. (1980). Spatiotemporal testing and modeling of catfish retinal neurons. *Biophys. J.* **29**, 13-36.
- Lasansky, A. and Marchiafava, P. L. (1974). Light-induced resistance changes in retinal rods and cones of the tiger salamander. *J. Physiol. (Lond.)* **236**, 171-191.
- Lasansky, A. and Vallerger, S. (1975). Horizontal cell responses in the retina of the larval tiger salamander. *J. Physiol. (Lond.)* **251**, 145-165.
- Lipetz, L. E. (1978). Information processing in the outer plexiform layer of the retina of cyprinid fish. Publ. 16, Inst. for Res. in Vision, Ohio State Univ.
- Marchiafava, P. L. and Pasino, E. (1973). The spatial dependent characteristics of the fish S-potentials evoked by brief flashes. *Vision Res.* **13**, 1355-1365.
- Marchiafava, P. L. and Torre, V. (1978). The responses of amacrine cells to light and intracellularly applied currents. *J. Physiol. (Lond.)* **276**, 83-102.
- Mitarai, G., Gato, T. and Tokagi, S. (1978). Receptive field arrangement of color-opponent bipolar and amacrine cells in the carp retina. *Sensory Processes* **2**, 375-382.
- Naka, K.-I. (1972). The horizontal cells. *Vision Res.* **12**, 573-588.
- Naka, K.-I., Marmarelis, P. Z. and Chan, R. Y. (1975). Morphological and functional identification of catfish retinal neurons III. Functional identification. *J. Neurophysiol.* **38**, 92-131.
- Naka, K.-I. and Ohtsuka, T. (1975). Morphological and functional identification of catfish retinal neurons. II. Morphological identification. *J. Neurophysiol.* **38**, 72-91.
- Naka, K.-I. and Rushton, W. A. H. (1967). The generation and spread of S-potentials in fish (Cyprinidae). *J. Physiol. (Lond.)* **192**, 437-461.
- Nelson, R. (1977). Cat cones have rod input: a comparison of the response properties of cones and horizontal cell bodies in the retina of the cat. *J. comp. Neurol.* **172**, 109-135.
- Neyton, J., Piccolino, M. and Gerschenfeld, H. M. (1981). Involvement of small-field horizontal cells in feedback effects on green cones of turtle retina. *Proc. Natl. Acad. Sci. USA* **74**, 4616-4619.
- Normann, R. and Perlman, I. (1979a) The effects of background illumination on the photoresponses of red and green cones. *J. Physiol. (Lond.)* **286**, 491-507.
- Normann, R. and Perlmann, I. (1979b). Signal transmission from red cones to horizontal cells in the turtle retina. *J. Physiol. (Lond.)* **286**, 509-524.
- Normann, R. A. and Werblin, F. S. (1974). Control of retinal sensitivity I. Light and dark adaptation of vertebrate rods and cones. *J. gen. Physiol.* **63**, 37-61.

- O'Bryan, P. M. (1973). Properties of the depolarizing synaptic potential evoked by peripheral illumination in cones of the turtle retina. *J. Physiol. (Lond.)* **235**, 207-223.
- Pasino, E. and Marchiafava, P. L. (1976). Transfer properties at rod and cone cells in the retina of the tiger salamander. *Vision Res.* **16**, 381-386.
- Piccolino, M., Neyton, J., and Gerschenfeld, H. (1981). Center-surround antagonistic organization in small-field luminosity horizontal cells of turtle retina. *J. Neurophysiol.* **45**, 363-375.
- Pinto, L. H. and Pak, W. L. (1974a). Light induced changes in photoreceptor membrane resistance and potential in Gecko retinas I. Preparation treated to reduce lateral interaction. *J. gen. Physiol.* **64**, 26-48.
- Pinto, L. H. and Pak, W. L. (1974b). Light-induced changes in photoreceptor membrane resistance in Gecko retinas II. Preparations with active lateral interactions. *J. gen. Physiol.* **64**, 49-69.
- Powers, R. L. and Arnett, D. W. (1981). Spatio-temporal cross-correlation analysis of catfish retinal neurons. *Biol. Cybern.* **41**, 179-196.
- Richter, A. and Simon, E. J. (1975). Properties of centre-hyperpolarizing, red-sensitive bipolar cells in the turtle retina. *J. Physiol. (Lond.)* **248**, 317-334.
- Richter, J. and Ullman, S. (1982). A model for the temporal organization of X- and Y-type receptive fields in the primate retina. *Biol. Cybern.* **43**, 127-145.
- Saito, T., Miller, W. H. and Tomita, T. (1974). C- and L-type horizontal cells in the turtle retina. *Vision Res.* **14**, 119-123.
- Schwartz, E. A. Responses of bipolar cells in the retina of the turtle, *J. Physiol. (Lond.)* **236**, 211-224.
- Shigematsu, Y., Yamada, M. and Fuwa, M. (1978). Latency measurement of the color coded S-potentials in the carp retina. *Vision Res.* **18**, 1435-1437.
- Siminoff, R. (1980a). Modeling of the vertebrate visual system I. Wiring diagram of the cone retina. *J. theor. Biol.* **86**, 673-708.
- Siminoff, R. (1980b). Modeling of the vertebrate visual system II. Application to the turtle cone retina. *J. theor. Biol.* **87**, 307-347.
- Siminoff, R. (1981). Modelling of the vertebrate visual system 3. Topological analysis of the cone mosaic. *J. theor. Biol.* **91**, 437-476.
- Siminoff, R. (1983a). An analogue model of the luminosity-channel in the vertebrate cone retina I. Hardware and responses to square wave voltages. *Biol. Cybern.* **46**, 101-110.
- Siminoff, R. (1984a). Systems analysis of an analogue model of the vertebrate cone retina. *IEEE Trans. on Systems, Man and Cybernetics SMC-13*, 1021-1028.
- Siminoff, R. (1984b). Electronic simulation of cones, horizontal cells and bipolar cells of the generalized vertebrate cone retina. *Biol. Cybern.* **50**, 173-192.
- Siminoff, R. (1984c). Influence of amacrine cells on receptive field organization of ganglion cells of the generalized vertebrate cone retina: electronic simulation. *Biol. Cybern.* **50**, 213-234.
- Siminoff, R. (1984d). Systems analysis of generalized vertebrate cone retina. Part A. Mathematical derivations. *J. theor. Neurobiol.* (preceding article).
- Simon, E. J. (1973). Two types of luminosity horizontal cells in the retina of the turtle. *J. Physiol. (Lond.)* **230**, 199-211.
- Simon, E. J. (1974). Feedback loop between cones and horizontal cells in the turtle retina. *Fed. Proc.* **33**, 1078-1082.
- Spekreijse, H. and Norton, A. L. (1970). The dynamic characteristics of color-coded S-potentials. *J. gen. Physiol.* **56**, 1-15.
- Teranishi, T., Negishi, K. and Kato, S. (1982). Two types of light-induced responses recorded from horizontal cells in the river lamprey retina. *Neurosci. Letters* **33**, 41-46.
- Tomita, T. (1978). Electrophysiological studies of retina cell function. *Invest. Ophthalm.* **15**, 171-187.
- Toyoda, J.-I., Saito, T. and Konda, H. (1978). Three types of horizontal cells in the stringray retina; their morphology and physiology. *J. comp. Neurol.* **179**, 569-580.
- Toyoda, J.-I. and Tonosaki, (1978). Studies on the mechanisms underlying horizontal-bipolar interaction in the carp retina. *Sensory Processes* **2**, 359-365.

- Tranchina, D., Gordon, J., Shapley, R. and Toyoda, J.-I. (1981). Linear information processing in the retina: a study of horizontal cell responses. *Proc. Natl. Acad. Sci. USA* **78**, 6540-6542.
- Vallerga, S., Cavacci, R. and Pottala, E. W. (1980). Artificial cone responses: a computer-driven hardware model. *Vision Res.* **20**, 453-457.
- Werblin, F. S. and Dowling, J. E. (1969). Organization of the retina of the mudpuppy, *Necturus maculosus* II. Intracellular recording. *J. Neurophysiol.* **32**, 339-355.
- Wu, S. M. and Dowling, J. E. (1980). Effects of GABA and Glycine on the distal cells of the cyprinid retina. *Brain Res.* **199**, 401-414.
- Wunk, D. F. and Werblin, F. S. (1979). Synaptic inputs to the ganglion cells in the tiger salamander retina. *J. gen. Physiol.* **73**, 265-286.
- Yang, X.-Li, Tauchi, M. and Kaneko, A. (1982). Quantitative analysis of photoreceptor inputs to external horizontal cells in the goldfish retina. *Jap. J. Physiol.* **32**, 399-420.
- Yazulla, S. (1976). Cone input to horizontal cells in the turtle retina. *Vision Res.* **16**, 727-735.